(12) INTERNATIONAL APPLICATION PUBLISHED UNDER THE PATENT COOPERATION TREATY (PCT)

(19) World Intellectual Property Organization
International Bureau

(43) International Publication Date
02 January 2025 (02.01.2025)

WIPO | PCT

(10) International Publication Number
WO 2025/002914 A1

(51) International Patent Classification:
A61K 31/13 (2006.01) *A61K 31/4725* (2006.01)
A61K 31/40 (2006.01) *A61P 9/10* (2006.01)
A61K 31/428 (2006.01)

(21) International Application Number:
PCT/EP2024/066950

(22) International Filing Date:
18 June 2024 (18.06.2024)

(25) Filing Language: English

(26) Publication Language: English

(30) Priority Data:
23382650.2 26 June 2023 (26.06.2023) EP

(71) Applicant: **CENTRO NACIONAL DE INVESTIGACIONES CARDIOVASCULARES CARLOS III (F.S.P.)** [ES/ES]; Melchor Fernández Almagro 3, 28029 Madrid (ES).

(72) Inventors: **MASTRANGELO, Annalaura**; Melchor Fernández Almagro 3, 28029 Madrid (ES). **ROBLES VERA, Iñaki**; Melchor Fernández Almagro 3, 28029 Madrid (ES). **SANCHO MADRID, David**; Melchor Fernández Almagro 3, 28029 Madrid (ES). **IBAÑEZ CABEZA, Borja**; Melchor Fernández Almagro 3, 28029 Madrid (ES). **FUSTER CARULLA, Valentín**; Melchor Fernández Almagro 3, 28029 Madrid (ES). **MAÑANES, Diego**; Melchor Fernández Almagro 3, 28029 Madrid (ES).

(74) Agent: **CLARKE, MODET Y CÍA., S.L.**; Calle Suero de Quiñones, 34-36, 28002 Madrid (ES).

(81) Designated States *(unless otherwise indicated, for every kind of national protection available)*: AE, AG, AL, AM, AO, AT, AU, AZ, BA, BB, BG, BH, BN, BR, BW, BY, BZ, CA, CH, CL, CN, CO, CR, CU, CV, CZ, DE, DJ, DK, DM, DO, DZ, EC, EE, EG, ES, FI, GB, GD, GE, GH, GM, GT, HN, HR, HU, ID, IL, IN, IQ, IR, IS, IT, JM, JO, JP, KE, KG, KH, KN, KP, KR, KW, KZ, LA, LC, LK, LR, LS, LU, LY,

(54) Title: ANTAGONISTS OF THE IMIDAZOLINE-1 RECEPTOR FOR USE IN THE PREVENTION AND/OR TREATMENT OF AN AUTOINFLAMMATORY OR AUTOIMMUNE DISEASE

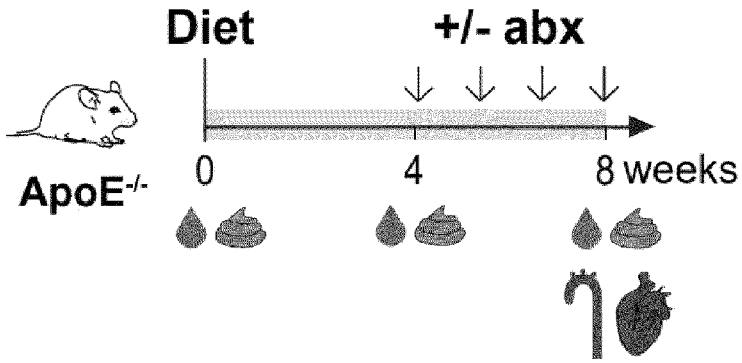

Figure 1a

(57) Abstract: The present invention refers to an antagonist of imidazoline-1 receptor (I1R) for use in the prevention and/or treatment of an autoinflammatory or autoimmune disease in a human subject, selected from the group consisting of (±)-2-endo-amino-3-exo- isopropylbicyclo[2.2.1]heptane (synonym: AGN192403), N-benzylguanidine, 2-(2- Fluoro-5-methylphenyl)-4,5-dihydro-1H-imidazole (synonym: S23757), 2-(2-chloro-4-iodo-phenylamino)-5-methyl-pyrroline (synonym: LNP911), 1-(4, 5-dihydro-1H-imidazol-2-yl)isoquinoline (synonym: BU98008), 5-[2-bromophenoxy)methyl]-4,5-dihydro-1,3- oxazol-2-amine (synonym: S23515), 6-methylamino-2methylheptene (synonym: isomethepteneٍ), and 4-chloro-2,3-dihydro-2-oxo-1,3-benzothiazol-3-ylacetic acid (synonym: benazolin). Also, to the use of Imidazole propionate in the diagnosis of an autoinflammatory or autoimmune disease in a subject, and further to a method of diagnosis of atherosclerosis comprising assessing the level of ImP in a blood sample and determining whether said level is above or below a value of 41nM.

WO 2025/002914 A1

[Continued on next page]

MA, MD, MG, MK, MN, MU, MW, MX, MY, MZ, NA, NG, NI, NO, NZ, OM, PA, PE, PG, PH, PL, PT, QA, RO, RS, RU, RW, SA, SC, SD, SE, SG, SK, SL, ST, SV, SY, TH, TJ, TM, TN, TR, TT, TZ, UA, UG, US, UZ, VC, VN, WS, ZA, ZM, ZW.

(84) **Designated States** *(unless otherwise indicated, for every kind of regional protection available)*: ARIPO (BW, CV, GH, GM, KE, LR, LS, MW, MZ, NA, RW, SC, SD, SL, ST, SZ, TZ, UG, ZM, ZW), Eurasian (AM, AZ, BY, KG, KZ, RU, TJ, TM), European (AL, AT, BE, BG, CH, CY, CZ, DE, DK, EE, ES, FI, FR, GB, GR, HR, HU, IE, IS, IT, LT, LU, LV, MC, ME, MK, MT, NL, NO, PL, PT, RO, RS, SE, SI, SK, SM, TR), OAPI (BF, BJ, CF, CG, CI, CM, GA, GN, GQ, GW, KM, ML, MR, NE, SN, TD, TG).

Declarations under Rule 4.17:

— *as to applicant's entitlement to apply for and be granted a patent (Rule 4.17(ii))*

Published:

— *with international search report (Art. 21(3))*

— *before the expiration of the time limit for amending the claims and to be republished in the event of receipt of amendments (Rule 48.2(h))*

— *in black and white; the international application as filed contained color or greyscale and is available for download from PATENTSCOPE*

ANTAGONISTS OF THE IMIDAZOLINE-1 RECEPTOR FOR USE IN THE PREVENTION AND/OR TREATMENT OF AN AUTOINFLAMMATORY OR AUTOIMMUNE DISEASE

Field of the Invention

The present invention is of application in the medical science, in particular in the diagnosis and treatment of autoinflammatory and autoimmune diseases, preferably atherosclerosis.

Background of the Invention

Cardiovascular diseases (CVDs) are the leading cause of death worldwide, with atherosclerosis (AT) being its main determinant. Despite advances in prevention and therapy, the proportion of the population living with disabilities and chronic illness after a cardiovascular event has risen over the years, highlighting the need to intervene early in the apparently healthy population.

At present, the identification and diagnosis of AT is mainly based on imaging examinations, being arteriography the gold standard for its diagnosis. However, although advances in medical imaging techniques have improved the detection of AT, the high cost and the challenges in large-scale screening has highlighted the need for cost-effective clinical markers to be used, optionally combined with other known AT risk factors.

Atherosclerosis is a chronic disease in which lipids build up in arteries causing local inflammation and the development of atheroma plaques. These plaques, which are infiltrated by immune cells, can impede blood flow and eventually cause blood clots due to their rupture leading to coronary artery disease or ischemic cerebrovascular disease.

Several biological mechanisms contribute to the etiology of AT, involving a combination of autoinflammatory and autoimmune factors. For instance, at early stages, macrophages take up (modified) low-density lipoprotein (LDL) that is retained in the arterial intima, causing intracellular lipid accumulation and macrophage foam cell formation. In plaques, macrophages can also show a proinflammatory phenotype that

promotes the secretion of cytokines and chemokines and amplifies the immune response by recruiting monocytes, T cells and neutrophils.

Recent research has challenged the notion of traditional risk factors, suggesting new players in the pathophysiology of AT that might be targeted to improve the efficiency of the therapy. Among them, accumulating evidence suggests that the microbiota-host metabolism crosstalk plays a central role in CVDs. However, despite the increasing literature on this topic, only a limited number of gut microbiota-dependent metabolites and mechanisms that underlie these correlations in atherosclerosis are described to date. Moreover, these studies are focused on more advanced stages of the disease where other risk factors may play a role, holding back the use of treatments targeting microbiota-dependent metabolites and stressing the importance of exploring earlier stages of the disease.

Imidazole propionate (ImP) is a downstream metabolite of histidine generated by the gut microbiota and associated with insulin resistance. Several non-patent documents have reported that the microbial metabolite ImP is present in patients and may contribute to the pathogenesis of type-2 diabetes (T2D), which is considered an inflammatory disease (Koh A. et al. Microbially Produced Imidazole Propionate Impairs Insulin Signalling through m TORC1, Cell 175, 947-961, 2018). It is important to note, though, that the etiology of AT and diabetes is not similar even if they may share some biological mechanisms. The fact that a metabolite is causal for diabetes does not imply *a priori* that is also causal for AT. There is no suggestion in this publication that ImP could play a similar role as proposed for diabetes in any inflammatory disease, even less in a disease combining an autoimmune etiology.

Molinaro has disclosed ImP associated with heart failure and mortality (Molinaro A. et al. Microbially Produced Imidazole Propionate is Associated with Heart Failure and Mortality, JACC Heart Failure, 2023, Article in press). The document is focused on prognosis and heart function. Heart failure is a clinical condition completely different from atherosclerosis; Diagnosis, prognosis, treatment, and causes of death are completely different between heart failure and atherosclerosis. There are very well-established biomarkers for heart failure (e.g. BNP) with no role at all in atherosclerosis, neither in subclinical stages nor in transition to acute coronary syndromes. On the other side, there are biomarkers well associated with atherosclerosis (e.g., LDL cholesterol) and with transition of atherosclerosis to acute coronary syndromes (e.g., CK MB) that have no

role at all in heart failure. Both conditions refer to the cardiovascular field but the fact that the metabolite is found in late stages of a disease does not imply that ImP can be *a priori* associated with early stages that may or not result on such a disease (in this case, atherosclerosis and heart failure). Therefore, the document does not teach or suggest the use of ImP as a biomarker for subclinical atherosclerosis.

US 2016/202239 A1 discloses extensive Figures of biomarkers associated with atherosclerotic coronary artery disease or plaques, amongst which ImP is cited. In this case, however, the inclusion of ImP should be considered speculative and beyond the experimental support of the publication; Describing the association of an increased value of ImP *versus* T2DM or AT is not equivalent to identifying the metabolite as a valid biomarker. In fact, the document does not show the corresponding Receiving Operating Characteristic (ROC) curve, although ROC curve analysis is generally considered as the standard method for biomarker performance assessment. ImP is rather listed as a metabolite significantly different between all Coronary Artery Disease (CAD) cases vs controls (Table 6, underlying statistic is a non-parametric test) and naïve CAD and controls (Table 10, underlying statistic is a non-parametric test) but, for instance, was not included in the Figures of metabolomics variables that are predictive for probability of CAD (Tables 11, 12, 15, 16, 20 & 21, underlying statistic is ROC curve analysis). Authors state that only the metabolomic variables predictive for probability of CAD should be included in the Figure of potential biomarkers of the disease, thereby teaching away from the use of ImP as biomarker for AT.

Lipid-lowering therapy has been used for decades in AT, with statins being the therapy of choice both in primary and secondary prevention for cardiovascular diseases. However, some subjects still have cardiovascular disease risk following statin therapy, despite achieving LDL-cholesterol targets. Alternative pharmacological agents have been proposed over the years to address this limitation, the majority of them targeting lipid metabolism and also anti-inflammatory drugs. However, the number of adverse effects, the cost and the need of parenteral administration have limited their use to specific cases and generally in combination with statins.

WO 2005/039639 A2 describe pharmaceutical compositions comprising selective imidazole receptor agonists combined with angiotensin II receptor blockers for the treatment of hypertension, especially in hypertensive patients already suffering from type II diabetes. A positive agonistic action on medullary I1R alone is sufficient to reduce

blood pressure. I1R agonists are involved in the inhibition of the sympathetic nervous system to inhibit vasomotor tone and thereby lowering the blood pressure. On the contrary, I1R-antagonist agents like AGN192403 provoke the opposite effect; although AGN192403 in particular is wrongly mentioned as an "agonist" in many references when in fact it is acting as "antagonist" (Head, G. A. & Mayorov, D. N. "Imidazoline receptors, novel agents and therapeutic potential" Cardiovasc. Hematol. Agents Med Chem. 4, 17-32, 2006). AGN192403 acting as ligand of I1R has no effect on blood pressure, let alone that a drug targeting hypertension should not be *a priori* related to atherosclerosis. Atherosclerosis cannot be confused with other cardiovascular pathologies that may be treated with anti-hypertensive agents; in fact, lipid-lowering therapies typically used for atherosclerosis would not have any effect on hypertension.

RU 2734281 C1 describes a composition for treating arterial hypertension and associated cardiovascular pathologies comprising a I1-imidazoline receptor agonist selected from moxonidine and rilmenidine, providing synergy with an β-adrenoreceptor blocking agent. The authors reported a more effective control of myocardial contractility and reduction of the risk of calcium overload of working cardiomyocytes, preventing the development of pathophysiological events in the heart. Moxonidine and rilmenidine are not selective for I1R, though, since they act through the α2-adrenergic receptor in the proposed mechanism. In any case and as stated above, the reported effect is achieved with a positive agonist effect on the receptor, whereas the document is silent about an eventual antagonist effect of a selective ligand to I1R.

The problem of the art can be formulated as providing a molecular way of treating autoimmune and autoinflammatory diseases, including atherosclerosis. The solution proposed by the present invention is the use of antagonists of the Imidazoline-1 receptor (I1R).

Description of the Invention

The present invention refers to an antagonist of imidazoline-1 receptor (I1R), or a pharmaceutically acceptable salt, tautomer, solvate, diastereomer, enantiomer, or prodrug thereof, wherein as valence and stability permit, for use in the prevention and/or treatment of an autoinflammatory or autoimmune disease in a human subject, in which said antagonist is (±)-2-*endo*-amino-3-*exo*-isopropylbicyclo[2.2.1]heptane (synonym: AGN192403), N-benzylguanidine, 2-(2-Fluoro-5-methylphenyl)-4,5-dihydro-1H-imidazole (synonym: S23757), 2-(2-chloro-4-iodo-phenylamino)-5-methyl-pyrroline

(synonym: LNP911), 1-(4, 5-dihydro-1H-imidazol-2-yl)isoquinoline (synonym: BU98008), 5-[2-bromophenoxy)methyl]-4,5-dihydro-1,3-oxazol-2-amine (synonym: S23515), 6-methylamino-2methylheptene (synonym: isometheptene), or 4-chloro-2,3-dihydro-2-oxo-1,3-benzothiazol-3-ylacetic acid (synonym: benazolin).

A preferred aspect of the invention is that said autoinflammatory or autoimmune disease is atherosclerosis.

In another preferred aspect, said human patient has a level of ImP in blood of at least 41nM, preferably between 41 nM and 266 nM.

Another aspect of the invention is a method of treatment of an autoinflammatory or autoimmune disease comprising administering an antagonist of the I1R in a patient in need thereof, preferably one of the antagonist compounds mentioned above.

Another preferred aspect is a pharmaceutical composition comprising an antagonist of I1R, in combination of at least one pharmaceutically suitable excipient.

Still a further aspect of the invention is a method for screening and/or producing therapeutic candidates for the prevention and/or treatment of an autoinflammatory or autoimmune disease, comprising in-vitro assessing whether a therapeutic candidate is able to inhibit the binding of ImP to I1R, wherein a positive result indicates that the therapeutic candidate is useful for the treatment of said autoinflammatory or autoimmune disease.

The present application confirms the microbial origin of ImP while revealing a direct correlation with increased atherosclerosis (Fig.1). This direct correlation of higher ImP metabolite in plasma with increased active subclinical atherosclerosis in healthy volunteers is also found in a human cohort (Fig. 2). In addition, the inventors have discovered that ImP is not only associated with atherosclerosis (AT) but is also causal for the progression of the disease (Fig 3).

The inventors have observed that ImP-induced atherosclerosis is associated systemically with increased inflammation and locally with an activation of fibroblasts, macrophages and endothelial cells in aorta (Fig 4). The mechanism of action of ImP further implicates a role in other autoimmune diseases by showing a remarkable enrichment of T cells and B cells in the aorta upon treatment with ImP (Fig 4). The data provided in the present application establish a clear link between ImP-induced AT and

the induction of innate and adaptive immune responses, strongly indicating a potential causal role for ImP in additional autoinflammatory and autoimmune diseases not limited to atherosclerosis.

ImP mediates its pro-atherogenic effect by acting on the I1R. The present invention demonstrates that ImP treatment triggered TNFα production and mTOR pathway activation in mouse aortic endothelial cells ECs (MAECs), bone marrow derived macrophages (BMDM) and in murine-embryonary fibroblasts (MEFs) (Fig.5). Stimulation of MAECs, BMDMs and MEFs with ImP in the presence of imidazoline receptor (IR) ligands showed that only AGN192403 (I1R antagonist) blocked the effect mediated by ImP (Fig.6). This indicates that ImP is a selective I1R endogenous ligand and that the binding ImP/I1R is blocked by treatment with AGN192403. Next, the inventors observed that blocking this ImP/I1R axis by the administration of AGN192403 induces a shift towards a less inflammatory environment both locally and systemically, preventing atherosclerosis development not only in response to ImP administration (Fig. 7) but also in response to high cholesterol diet (Fig. 8), a diet that elevates ImP levels in blood (Fig 1g).

Through the identification of the ImP receptor, the present invention describes a novel therapy based on the blockage of this axis that is able to prevent atherosclerosis and, more remarkably, to treat it independently of the metabolism of lipids, the established risk factor for atherosclerosis (Fig.7 and 8).

The present invention refers to compounds as selective ligands for I1R that therefore do not or only scarcely interact with α2-adrenoreceptor and I2R for the treatment of atherosclerosis and other autoimmune and autoinflammatory diseases. In addition, the compounds have to be antagonists of I1R.

In the present invention, a “ligand of the receptor” is understood to be an inorganic or organic molecule capable of interacting and of antagonist effect on the activation of the receptor, or any other agent capable of negatively impacting the biological function of the receptor.

In the present invention, a “selective ligand” is understood to be a ligand acting directly in the receptor while maintaining selectivity over potential off-targets.

Another aspect of the invention proposes a personalized therapy based on the identification of individuals with high levels of ImP in the blood that are more likely to benefit from the inhibition of this specific axis. Indeed, it has been observed that ImP levels are significantly increased in subjects with subclinical AT when compared to controls. Moreover, higher levels of ImP in the bloodstream were also associated with increased risk of having AT, which held true after adjusting for traditional risk factors, including total cholesterol, hypertension, current smoking, among others (Fig. 2). This additionally indicates that the ImP level in bloodstream can serve as a biomarker of subclinical AT.

The inventors further describe the discriminative performance of ImP to detect early AT when the ImP is considered alone or combined with features associated with AT (i.e., familial hypercholesterolemia, familiar history of cardiovascular disease, active smoking, hypertension, hemoglobin and creatinine in blood) (Fig. 2). Notably, ImP performed better in discriminating subjects with early AT when compared to markers and scores routinely used in the clinics (e.g., LDL-cholesterol in blood and others) (Fig. 2), even in terms of sensitivity and specificity when the clinically recommended cut-off is used.

Another aspect of the invention is the use of ImP in the diagnosis of an autoinflammatory or autoimmune disease in a biological sample obtained from a subject, preferably AT.

In a preferred aspect, said biological sample is a is a blood sample or a plasma sample.

Another preferred aspect of the present invention is a method of diagnosis of AT, comprising assessing the level of ImP in a blood or plasma sample obtained from a human subject, and determining whether said level is above or below a value of 41nM, wherein a value above 41nM is indicative of likelihood of having early AT.

In a more preferred aspect, said level of ImP is between 41 and 266 nM.

Still another aspect of the invention is a method of detecting ImP in a blood or plasma sample obtained from a subject having or at risk of an autoinflammatory or autoimmune disease, preferably AT, the method comprising detecting a level of ImP in a blood or plasma sample collected from the subject and determining whether the level of ImP is above or below a value of 41nM.

In a preferred aspect of the invention, said method is liquid chromatography coupled with mass spectrometry (LCMS).

In the scope of the present invention, the term “diagnosis” is understood as the prediction of atherosclerosis when no symptoms are yet detectable in a healthy subject.

Metabolite cut-off values were derived for ImP by the ROC curves analysis. Based on this, the invention includes a method of diagnosing the subject as being more likely to have AT by assessing the level of ImP in a blood sample of said subject, and determining whether said level in the bloodstream is above or below a value of 41nM, wherein a value above 41nM is indicative of the subject more likely having early AT. ImP is associated with and can be complementary to features of early atherosclerosis.

Therefore, another preferred aspect of the invention is the use of ImP in combination with other risk factors to diagnose atherosclerosis at a subclinical stage where the confounding effects of other comorbidities are limited. In addition to ImP, other biological variables to count on are familiar history of CVDs, hypertension, current smoking, hemoglobin, creatinine and familial hypercholesterolemia.

Brief description of the Figures

Figure 1 shows how ImP is associated with atherosclerosis in ApoEKO mice.

Figure 1a - ApoEKO male (8 weeks old) mice were fed different diets (chow, high cholesterol (HC), and HC & high choline (HC/HC) for 8 weeks. At 4 weeks post diet initiation, a cocktail of antibiotics (abx) including ampicillin (1mg/ml), neomycin (1mg/ml), metronidazole (1mg/ml) and vancomycin (0.5mg/ml) was added (or not) in the drinking water to deplete microbiota.

Figure 1b - Atherosclerotic plaque lesion size was increased in ApoEKO mice fed HC diets (10% fat, 0.75% cholesterol), in a microbiota-dependent manner in the HC/HC (HC+ 1% choline) diet. Aortic lesion was quantified by oil red O staining. Data from two independent experiments (n=10 in each group).

Figures 1c to 1f - Unbiased metabolomics shows that gut microbiota modulation by diet and abx is associated with changes in the plasma metabolome of ApoEKO mice. Score plot of the PLS-DA analysis performed on LC(HILIC)-MS ESI+ data of plasma samples collected at culling (n=10 in each group). (c) PLS-DA score plot generated from the comparison between the three different diets (♦Chow, ■HC and ▲HC/HC) (PC1= 16.8, PC2=9.2). (d) PLS-DA score plot generated from the comparison between ♦chow vs

♦chow+abx. (PC1= 15.6, PC2=7.1). (e) PLS-DA score plot generated from the comparison between ■HC vs ▩HC+abx. (PC1= 14.1, PC2=35.5). (f) PLS-DA score plot generated from the comparison between ▲HC/HC vs ◭HC/HC+abx. (PC1= 13.7, PC2=29.2).

Figure 1g - The relative abundance of Imidazole propionate (ImP) was determined by LC-MS unbiased metabolomics analysis of plasma collected from ApoEKO male mice at sacrifice, showing ImP as a microbiota-dependent metabolite.

Figure 1h - ImP abundance correlates with aortic lesion. Correlation coefficient r = +0.73 and p<0.0001 are calculated as the Pearson's parametric correlation test.,

Figure 1i - Tandem mass spectrometry fragmentation by higher-energy collisional dissociation (HCD) using 50eV as collisional energy of an authentic imidazole propionate (ImP) standard (left, top) and endogenous m/z = 141.06535 mass from plasma of ApoE-/- mice fed HC diets (left, middle and bottom), HC/HC diet and abx (right, middle) or chow (bottom, right). Arithmetic mean± SEM of each group is shown. ∗p< 0.05, ****p<0.0001 vs. control (the same diet without abx) ##p< 0.01, ####p< 0.0001 vs. chow diet by one-way ANOVA (Tukey correction

Figure 2 shows how ImP is increased in subjects with subclinical atherosclerosis.

Figures 2a, 2b - Plasma levels of ImP in healthy subjects (n=105) and subjects with subclinical atherosclerosis (n=295). Subjects with subclinical atherosclerosis (AT) were further stratified according to vascular inflammation (arterial 18F-FDG uptake, AT_FDG, n=57), bone marrow (BM) activation (18F-FDG uptake in BM, AT_BM, n=40), systemic inflammation (concurrent arterial and BM FDG uptake, AT_SYS, n=124) and inactive AT (no 18FDG uptake in any compartment, AT_I, n=74). Arithmetic mean± SEM of each group is shown. **p<0.005, vs. healthy subjects by Mann–Whitney U test.

Figure 2c - Multinomial logistic regression for subclinical AT (both for all subjects with AT and for each subgroup of AT considered individually) vs. healthy controls according to ImP. Model 1 OR was adjusted for age, sex and active smoking. Model 2 was adjusted for Model 1 plus glucose (fasting), high-sensitivity C-reactive protein and hemoglobin levels. Squares represent OR and the upper and lower whisker the 95 % confidence

intervals (CI), *p < 0.05, **p < 0.01, ***p < 0.001. □ Unadjusted, ▒ Model 1, ■ Model 2.

Figures 2d to 2i - ROC-AUC statistics of (d) ImP (AUC:0.582, CI:0.520-0.644), Cutoff: 41 nM, Sensitivity: 0.287, Specificity: 0.848, (e) a ImP-Panel based LASSO regression model (AUC:0.751, CI:0.673-0.788), (f) LDL-C (AUC:0.534, CI:0.469-0.598), Cutoff: 160 mg/dL, Sensitivity: 0.208, Specificity: 0.838, (g) Total cholesterol (AUC:0.542, CI:0.481-0.61), Cutoff: 240 mg/dL, Sensitivity: 0.194, Specificity: 0.838, (h) HDL-C (AUC:0.527, CI:0.462-0.586) Cutoff: 40 mg/dL, Sensitivity: 0.136, Specificity: 0.867, and (i) SCORE model (AUC:0.68, CI:0.622-0.737) for detection of early AT. Variables in the Figure are ImP, FHCVD, HTN, current smoking, hemoglobin, creatinine and familial hypercholesterolemia. Abbreviations: BP, blood pressure; hs-CRP, high-sensitive C-reactive Protein; FHCVD, Familial History of CVDs, HTN, hypertension.

Figure 3 shows how ImP is able to induce atherosclerosis.

Figure 3a - ImP supplementation to the drinking water (400 µg/mouse/day) induces AT in $ApoE^{-/-}$ male mice that were fed chow diet for 8 weeks (+/- ImP) after weaning Aortic lesion was quantified by oil red O staining. Data are pooled from two independent experiments, n=13-14, ▒Chow, ▓ Chow-ImP.

Figure 3b - Total Cholesterol, and LDL cholesterol levels in plasma from $ApoE^{-/-}$ mice treated with ImP fed with chow diet for 8 weeks. Data are pooled from two independent experiments, n=14.

Figure 3c - ImP supplementation to the drinking water (400 µg/mouse/day) induces AT in $LDLr^{-/-}$ male mice that were fed chow diet for 12 weeks (+/- ImP) after weaning. Aortic lesion was quantified by oil red O staining. Data are pooled from 2 independent experiments, n=10, ▒Chow, ▓ Chow-ImP.

Figure 3d - Arithmetic mean± SEM and individual data of each group are shown. Total cholesterol, and LDL levels in plasma from $LDLr^{-/-}$ mice treated with ImP and fed with chow diet for 12 weeks. Data are pooled from 2 independent experiments n=9-10. Arithmetic mean± SEM of each group is shown. *p<0.05; **p<0.01 vs. control

Figure 4 shows how ImP induces innate and adaptive responses that promote inflammation and immunity.

Figure 4a - Ly6C^{high} monocytes and T cell subpopulation (Th1 and Th17) from blood of ApoE$^{-/-}$ male mice that were fed chow diet for 8 weeks (+/- ImP) after weaning. Compared treated with ImP or not treated. The mean ± SEM from two independent experiments, n=7-8.

Figure 4b - mTOR (pS6) activation on peritoneal macrophages from Apoe-/- mice treated as in a, quantified by flow cytometry.

Figure 4c - UMAP embedding of whole aorta-derived cells based on transcriptomic profiles after 8 weeks under chow diet (control) or chow diet + ImP (ImP) colored by cell type.

Figure 4d - Cell proportions obtained from scRNA-seq data comparing control vs ImP conditions.

Figure 4e - Immune cells proportions obtained from scRNA-seq data and flow cytometry comparing control vs ImP conditions.

Figure 4f - Heat map of Gene set enrichment analysis (GSEA) for Macrophages (MFs), Fibroblasts (FBs) and endothelial cells (ECs). Kolmogorov Smirnov test was performed. Unpaired Student's t test between Ctrol and ImP; *p< 0.05; **p<0.01, unless otherwise stated.

Figure 5 shows how mTOR activation in immune cells contributes to ImP-induced inflammatory response and atherosclerosis.

Figures 5a, 5b - Mouse aortic ECs (MAECs), murine-embryonary fibroblasts (MEFs) and bone marrow derived MFs (BMDM) were treated 24h in vitro with ImP (ImP, 10 µg/mL) or not (Ctrol) co-incubated with Rapamycin (10nM). a, TNFα production from mouse MAECs, MEFs, BMDM, measure in the supernatant of stimulated cells and quantified by ELISA. b, Phospho-S6 activation measured by flow cytometry MFI. Four independent experiments in MAECs, nine in MEFs, and seven in BMDM. One-way ANOVA was performed (Tukey correction).

Figure 5c - LDLr$^{-/-}$ male mice, were lethally irradiated, and grafted with bone marrow harvested from LysMcreRaptor mice Cre+ or Cre-. After 60 days grafted mice were supplemented in the drinking water with ImP (400 µg/mouse/day) for 12 weeks and fed with chow diet. ▒ Chow, ▓ Chow-ImP

Figure 5d - ImP supplementation to the drinking water (400 µg/mouse/day) was unable to induce AT in LDLr$^{-/-}$ male mice grafted with BM from LysMcreRaptorCre^{+} mice. Aortic lesion was quantified by oil red O staining. Data are pooled from one experiment, n=7-9. Unpaired Student's t test between Ctrol and ImP; *p< 0.05; **p<0.01; ***p<0.005; ****p<0.0001, unless otherwise stated.

Figure 6 shows how Imidazoline 1 receptor activation mediated the proinflammatory profile generate by ImP on several cell types. Figures a, b provide graphs showing the key role of mTOR activation and Imidazoline 1 receptor as clue in the in vitro induction of proinflammatory cytokines and mTOR activation induce by ImP in several cell types.

Figures 6a, 6b - Mouse aortic ECs (MAECs), bone marrow derived MFs (BMDM) and in murine-embryonary fibroblasts (MEFs) were treated in vitro with ImP (ImP, 10 µg/mL) or not (Ctrol) co-incubated with Rapamycin (10nM, mTOR1 antagonist) AGN192403 (10 µg/mL, I1R antagonist), Idazoxan (0.06 µg/mL, IR and α2 antagonist) or Yohimbine (1 µg/mL, α2 antagonist). Rapamycin and AGN192403 co-incubations were able to block the induction of TNFα production and Phospho-S6 activation induce by ImP. Data are pooled from n=4 independent MAECs, n=9-10 to MEF, and n=7-12 to BMDM cultures. Arithmetic mean± SEM and individual data of each group is shown. * p<0.05, **p<0.01, ***p<0.005, **** p<0.0001 one-way ANOVA (Tukey correction).

Figure 7 shows how ImP mediates its effect on atherosclerosis through the imidazoline receptor 1. Figures a, b provide evidence showing the key role of Imidazoline 1 receptor *in vivo* as mediator of atherogenic plaque induced by ImP, and the independency of changes in total cholesterol and Ldl cholesterols in this effect. Figures c-e show the clue role of Imidazoline 1 receptor in the systemic inflammation induce by ImP, determinate by the reduction of proinflammatory cells population, Figure a, the blocking of increase of proinflammatory cytokines, Figure d, and the prevention of mTOR pathway activation in macrophages, Figure e. Figures f, g show the capacity of Imidazoline 1 receptor to mediate the aorta inflammation induce by ImP,

Figure 7a - ApoE$^{-/-}$ male mice that were fed chow diet for 8 weeks were supplemented in the drinking water with ImP (400µg/mouse/day) and AGN192403 (30µg/mouse/day). Aortic lesion was quantified by oil red O staining. AGN192403 treatment prevented the ImP atheroma plaque induction. Data are pooled from three independent experiments, n=15-17.

Figure 7b - Total Cholesterol, and LDL levels in plasma from ApoE$^{-/-}$ mice treated with ImP and ImP+AGN192403 fed with chow diet for 8 weeks. Data are pooled from three independent experiments, n=13-20.

Figure 7c - Ly6C^{high} monocytes, and Th1 cell on blood, from ApoE -/- mice treated 8 weeks with ImP +- AGN192403 on the drinking water. Data are pooled from three independent experiments, n=15.

Figure 7d - INFγ and TNFα cytokine concentration measured by ELISA in plasma from ApoE$^{-/-}$ mice treated 8 weeks with ImP +- AGN192403 on the drinking water Two pooled experiments, n=10.

Figure 7e - Phosphorylation of the s6 in peritoneal macrophages harvested from ApoE$^{-/-}$ mice treated 8 weeks with ImP +- AGN192403 on the drinking water, measure by flow cytometry. Two pooled experiments, n=10. f-g,

Figure 7f, 7g - Th1/Treg ratio and b) changes in Th1 and Treg population infiltrated in aorta in ApoE -/- mice treated with ImP +- AGN 192403 fed with chow diet for 8 weeks. n=7-9. Individual data and mean ± SEM from indicated independent experiments is shown unless otherwise stated. One-way ANOVA was performed (Tukey correction). * $p < 0.05$; ** $p < 0.01$; *** $p < 0.005$.

Figure 8. shows how the inhibition of the I1R/ImP pathway prevents atherosclerosis progression. Figures a, b provide evidence showing Imidazoline 1 receptor blocking *in vivo* as target receptor to atherogenic plaque induce by High Cholesterol diet, and the independency of changes in total cholesterol and Ldl cholesterols in this effect. Figures c-f show Imidazoline 1 receptor as a target to reduce the systemic inflammation in AT: Figures c-d, determined by the reduction of proinflammatory cells population; Figure e, the reduction of proinflammatory cytokines; and Figure f, the reduction of mTOR pathway activation in macrophages.

Figures 8a, 8b - ApoE$^{-/-}$ male (8 weeks old) mice were fed different diets (chow, high cholesterol (HC 10% fat, 0.75% cholesterol) for 8 weeks. At 4 weeks post diet initiation, AGN192403 (30 µg/mouse/day) was administrated in the drinking water until week 8. Aortic lesion was quantified by oil red O staining. Data from two independent experiments, n=13-15. 8b - Total Cholesterol, and LDL cholesterol levels in plasma from treated mice, n=15.

Figures 8c, 8d - Number of Ly6C^{high} (c) and th1 (d) cells from blood, analyzed by Flow Cytometry from ApoE$^{-/-}$ male (8 weeks old) mice were fed different diets (chow, high cholesterol) for 8 weeks. At 4 weeks post diet initiation, AGN192403 was administrated in the drinking water until week 8. Data are pooled from two independent experiments n=9-13.

Figure 8e - Proinflammatory cytokines INFg production was measured by ELISA from plasma of ApoE$^{-/-}$ male (8 weeks old) mice were fed different diets (chow, high cholesterol) for 8 weeks. At 4 weeks post diet initiation, AGN192403 was administrated in the drinking water until week 8. Data are pooled from two independent experiments n=10.

Figure 8f - mTOR (pS6) activation on peritoneal macrophages from ApoE$^{-/-}$ male (8 weeks old) mice were fed different diets (chow, high cholesterol) for 8 weeks. At 4 weeks post diet initiation, AGN192403 was administrated in the drinking water until week 8, quantified by flow cytometry. Data are pooled from two independent experiments n=10-12. Individual data and mean ± SEM from indicated independent experiments is shown unless otherwise stated. One-way ANOVA was performed (Tukey correction). * $p < 0.05$; ** $p < 0.01$; *** $p < 0.005$; **** $p < 0.001$.

Examples

Example 1. Unbiased metabolomics reveals ImP as a metabolite associated with atherosclerosis

To study how microbiota may affect atherosclerosis (AT) we fed ApoE-KO mice (8 weeks old) different diets: chow, high cholesterol (H, 10% fat, 0.75% chol) and HC-high choline (HC/HC, HC+ 1% choline) for 8 weeks. Treatment with a cocktail of antibiotics (abx) including ampicillin (0.5 mg/ml), gentamicin (0.5 mg/ml), metronidazole (0.5 mg/ml), neomycin (0.5 mg/ml), and vancomycin (0.25 mg/ml) dissolved in the drinking water depleted the majority of the mouse microbiota. Plasma samples were collected at different times after overnight fasting, and the heart and aorta at sacrifice as indicated (Fig.1. Figure a).

For atherosclerotic lesion measurements, mice were perfused with 10 ml of Phosphate Buffered Saline (PBS) via cardiac puncture to remove blood contamination from vascular tissue. The aortas were dissected and fixed in formaldehyde 4% w/w (PanReac,

AppliChem) overnight. Then, the exposed aortas were stained for lipid depositions with Oil Red O (Sigma-Aldrich), and an end face assay was performed. Images were taken with a Leica Nikon camera magnifier and an atherosclerotic lesion in the aorta was measured using ImageJ software. HC diets (HCDs) induced atherosclerosis, which in the HC/HC group was significantly reduced in the presence of abx (Fig.1. Figure b), suggesting that AT progression in this model depends on microbiota.

The host plasma metabolome was analyzed by untargeted metabolomics to identify novel metabolites associated with AT and/or microbiota. Specifically, proteins were removed from plasma samples, which were collected at culling, by adding a cold (-20°C) mixture of Methanol:Ethanol (1:1, v/v) in a ratio 5:1 (solvent:sample) and by storing the samples on ice for 20 minutes. Blank sample was prepared following the same extraction procedure, adding only the solvents to a 1.5 mL Eppendorf tube. Samples and blank were centrifuged at 16400 g for 20 minutes 4°C and the supernatant was transferred in a 1.5 mL Eppendorf tube. Supernatants were subsequently dried-out in speedvac (Savant SPD131DDA concentrator, Savant RVT5105 refrigerated vapor trap and OFP400 vacuum pump, ThermoFisher Scientific, Waltham, Massachusetts, USA) for 2 hours at room temperature. Before LC-MS analysis, the dried samples were resuspended in 50µL of a mixture composed of ACN:H2O (90:10, v:v) by constant shaking at 1000 rpm for 10 min at 8°C and then centrifuged at 16400 g for 5 minutes to remove insoluble material. The soluble part was placed in the insert of the LC–MS vial.

Metabolomics untargeted analysis was performed using a Ultimate 3000 HPLC system consisting of a degasser, two binary pumps, and thermostatic autosampler, maintained at 8°C (ThermoFisher Scientific) coupled to a LTQ Orbitrap XL™ Hybrid Ion Trap-Orbitrap Mass Spectrometer (ThermoFisher Scientific). 5 µL of the samples were injected onto a Merck SeQuant ZIC-HILIC column (150 × 1 mm, 3.5 µ), which was settled at 45°C, and metabolites were eluting at 180 µL/min with solvent A composed of water with 0.1% formic acid, and solvent B composed of acetonitrile with 0.1% formic acid. The gradient started from 90% to 25% of B in 15 min, keeping constant for 3 min and returned to starting conditions in 0.1 min, finally by keeping the re-equilibration at 90% of B for 11.9 min. Data were collected in positive ESI ion mode. The MS was operating in full scan mode from 70 to 1000 m/z at 60000 resolution. MS/MS spectra were collected in data-dependent mode via higher-energy C-trap dissociation (HCD) in the orbitrap. Samples were analyzed in a randomized order.

Generated data was firstly aligned using Compound Discoverer (ThermoFisher Scientific); signals were extracted and grouped into features (isotopic traces from a single analyte at a particular charge state) using the Metaboprofiler node in Compound discoverer (the open-source plug-in freely available from OpenMS (Röst HL, et al. OpenMS: a flexible open-source software platform for mass spectrometry data analysis. Nat Methods. 30;13(9):741-8, 2016). Features were then filtered by presence keeping the entities that were present at least in the 80% of the samples from the same group. Afterwards, missing values were imputed using the KNN method or by LoDs (1/5 of the minimum positive value of each variable) according to the % of missing values of the feature within the group in MetaboAnalyst (Chong J, et al. Using MetaboAnalyst 4.0 for Comprehensive and Integrative Metabolomics Data Analysis. Curr Protoc Bioinformatics. 68(1):e86, 2019).

Data was autoscaled and log transformed before applying a multivariate data analysis (i.e., partial least squares discriminant analysis, PLS-DA) to assess changes in the metabolome that depended on the diet or the absence of the microbiota (Fig.1. Figures c-f). Metabolites were annotated by searching the accurate mass against the Ceu Mass Mediator (Gil-de-la-Fuente A, et al. CEU Mass Mediator 3.0: A Metabolite Annotation Tool. J Proteome Res. 1;18(2):797-802, 2019) and the resulting data matrix handled by Turboputative (Barrero-Rodríguez R, et al. Turboputative: A web server for data handling and metabolite classification in untargeted metabolomics. Front Mol Biosci. 8;9:952149, 2022).

Following this analysis, Imidazole propionate was revealed as a microbiota-dependent - metabolite (Fig.1. Figure g) that positively correlated with atherosclerosis (Fig.1. Figure h). The annotation of ImP was confirmed by MS/MS spectra comparison between the experimental feature corresponding to ImP and its standard both acquired in a subsequent LC/MS/MS analysis that was carried out using the same chromatographic conditions outlined previously (Fig.1. Figure i).

Example 2: ImP is a biomarker of early atherosclerosis in humans

To test whether plasmatic ImP is associated with atherosclerosis in humans, a sub-cohort of volunteers was selected from the PESA-CNIC-Santander prospective cohort study (n=4,194 subjects of 40 to 54 years of age and free of known CVD at baseline). This cohort consisted of 400 asymptomatic volunteers with a median age of 57 years (interquartile range (IQR) 54-59), of whom 78.2% were male and 24% current smokers,

and without diabetes to exclude the confounding effect of ImP promoting insulin resistance (Table 1). Based on multi-territorial/multimodal imaging (i.e., 2D/3D vascular ultrasound and non-contrast computed tomography), 295 participants were classified with subclinical atherosclerosis and 105 controls as described previously (Fernández-Friera L, et al. Prevalence, Vascular Distribution, and Multiterritorial Extent of Subclinical Atherosclerosis in a Middle-Aged Cohort: The PESA (Progression of Early Subclinical Atherosclerosis) Study. Circulation. 2015 Jun 16;131(24):2104-13). Subjects with early atherosclerosis were further stratified according to their metabolic activity that was measured by active uptake of Fluorodeoxyglucose (^{18}F-FDG) in bone marrow (AT_BM, n=40), arteries (AT_AFDG, n=57), in both compartments (AT_SYS, n=124) or in none (AT_I, n=74) as described previously (Fernández-Friera L, et al. Vascular Inflammation in Subclinical Atherosclerosis Detected by Hybrid PET/MRI. J Am Coll Cardiol. 2019 Apr 2;73(12):1371-1382) (Devesa A, et al. Bone marrow activation in response to metabolic syndrome and early atherosclerosis. Eur Heart J. 2022 May 14;43(19):1809-1828).

LC-MS-based targeted metabolomics was used to quantify ImP and its related metabolites (i.e., histidine and urocanic acid) in plasma samples. Specifically, proteins were precipitated by adding a cold (-20°C) mixture of Methanol:Ethanol (1:1, v/v) in a ratio 2:1 (solvent:sample) and by storing the samples on ice for 20 minutes. Samples were centrifuged at 16400 g for 20 minutes 4°C and the supernatant was transferred in in the insert of the LC–MS vial.

Data was acquired by using an HPLC system 1290 Infinity series coupled to a triple quadrupole (QqQ) 6460 MS from Agilent Technologies. 1 uL of the sample in Methanol:Ethanol was injected onto an InfinityLab Poroshell 120 HILIC-Z column (2.7 um 150 x 2.1 mm, Agilent Technologies, Santa Clara, California) with a flow rate of 0.50 mL/min. Mobile phase A contained 20 mM ammonium formate in ultrapure water at pH 3, whereas mobile phase B contained 20 mM aqueous ammonium formate at pH 3 in ACN/H20 (9:1, v/v). The initial conditions at time 0 were 100% B, decreasing to 70% at 11.5 min. The gradient was then increased to 100% B at time 12.0 min and held until the total run time of 15 min. Raw signals for multiple reaction monitoring (MRM) transitions were checked and peaks corresponding to all the targeted compounds were integrated by MassHunter Quantitative B.10.00 (Agilent Technologies). Multiple reaction monitoring transitions (collision energy, eV) were as follows: 141>123 (10) and 141>81 (26) for ImP; 139>121 (10) and 139> 93 (26) for urocanic acid; 142>124 (10) and 142> 41 (26) for labeled urocanic acid; 156>110 (10) and 156 > 83 (30), for histidine; and, 159>113 (10)

and 159 > 86 (30) for labeled histidine. Quantification of ImP concentration was performed by generating a standard curve with known concentrations of this metabolite. Histidine and urocanic acid were instead quantified by using internal standards added to the plasma samples as stated above. Metabolite standards were analyzed alongside the plasma samples using the LC-MS/MS method. The dilution of the plasma during the sample preparation was also considered for the quantification.

Authors found that ImP levels were significantly increased in subjects with subclinical atherosclerosis when compared to controls, but not histidine or urocanic acid levels (Fig. 2a-c). Moreover, a higher concentration of ImP was associated with increased risk of having AT calculated using multinomial logistic regression. Odds ratio and confidence (CI) interval were provided showing that increased ImP levels were significantly associated ($P<0.05$) with higher risk of AT also after adjusting for AT traditional risk factors (Fig. 2c). Remarkably, in our cohort, ImP levels were more strongly associated with active rather than inactive AT, with AT_BM and AT_SYS being the groups with the strongest association between ImP and increased risk of AT (Fig. 2b-c).

Finally, ROC curve analysis was used to assess the discriminative performance of ImP to diagnose a subject more likely to have subclinical AT. Specifically, ImP showed an AUROC equal to 0.58 (95% confidence interval (CI): 0.52-0.64, $P<0.01$) (Fig. 2d) that increased up to 0.75 (95% CI: 0.70-0.80, $P<0.0001$) when ImP is combined with features selected according to the LASSO method (i.e., familial hypercholesterolemia, familiar history of cardiovascular disease, active smoking, hypertension, hemoglobin and creatinine in blood) (Fig. 2e). Of note, ImP performed better in discriminating subjects with early atherosclerosis when compared to markers routinely used in the clinics such as LDL-cholesterol in blood (AUC=0.53, 95% CI:0.47-0.60, P=0.19) and others (Fig. 2 f-h), even in terms of sensitivity and specificity when the clinically recommended cut-off is used, as well as when compared to the standard SCORE2[2] (AUC=0.68, 95% CI:0.62-0.74, $P<0.0001$) (Fig. 2i).

Example 3: ImP is able to induce atherosclerosis

To deepen into the role of ImP on atherosclerosis and determine whether ImP has a direct causal role on the disease etiology, ImP (400ug/mL) was supplied in the drinking water of chow-fed *ApoE*$^{-/-}$ mice for 8 weeks. After treatment, blood was collected, and mice were perfused with 10 ml of Phosphate Buffered Saline (PBS) via cardiac puncture to remove blood contamination from vascular tissue. The aortas were dissected and fixed

in formaldehyde 4% w/w (PanReac, AppliChem) overnight. Then, the exposed aortas were stained for lipid depositions with Oil Red O (Sigma-Aldrich), and an *en face* assay was performed. Images were taken with Leica Nikon camera magnifier and atherosclerotic lesion in the aorta measured using ImageJ software (Fig 3a). The effect on the cholesterol or lipoprotein levels in blood were analyzed with a Dimension RxL Max automated analyzer the day after the extraction, no changes were found (Fig. 3b). These results were also confirmed in *Ldlr* $^{-/-}$ mice fed a chow diet and treated with ImP for 12 weeks (Fig. 3c-d), revealing ImP as a novel contributor to atherosclerosis etiology even in a model of atherosclerosis that requires the use of a high cholesterol/fat diet to induce the disease.

Example 4: ImP induces innate and adaptive responses that promote inflammation and immunity.

The effect of ImP on the immune cells were analyze by flow cytometry (FACS). Single cells blood suspension was stained for 30 min at 4°C with LIVE/DEAD Fixable Aqua Dead Cell Stain Kit (Life Technologies). After washing with PBS, cells were stained in FACS buffer containing anti-CD16/32 (BioXcell), 3% FBS and 0.05% EDTA with the corresponding antibody cocktail for 30 min on ice. ImP induced an expansion of pro-inflammatory Ly6C^{hi} monocytes (CD45+Ly6C+), T-helper 17 (Th17) (CD90+CD4+Rorg+) and Th1 cells (CD90+CD4+T-bet+) (Fig. 4a) in the blood. In addition, the systemic inflammation was validated analyzing the S6 ribosomal protein phosphorylation (pS6) by FACS which is a marker of mTOR activation (Fig 4b). These changes which have been shown to promote a pro-atherogenic environment, suggesting a systemic inflammation that is driven by ImP and is associated with atherosclerosis development.

Next, to comprehensively distinguish the ImP-mediated local changes in the aorta, a single-cell RNA sequencing (scRNA-seq) analysis of the whole aorta was performed from chow-fed *ApoE*$^{-/-}$ mice administered ImP for 4 or 8 weeks. The aortas were collected and kept in cold Dulbecco's Modified Eagle Medium (DMEM) to be digested. Perivascular fat was removed and the thoracic aortic with arch was open longitudinally and chopped. The chopped aorta was incubated for 30 min at 37ºC in water bath in digestion buffer (Collagenase A (25 mg/ml), (Roche/Sigma #10103586001). Dispase II (25 mg/ml), (Roche/Sigma #04942078001), DNase I (250 µg/ml) (Roche/Sigma #10104159001) elastase (25ul/ml) and Liberase TL (0.2 Wünsch units/mL) Cat#

5401119001. After incubation time the digested tissue was mixed by pipetting, filtered through a 70um strainer and spinned at 400g 5 min 4ºC. To get enough cells numbers, 3 aortas per condition were pooled.

Each sample was labeled with a cell multiplexing oligo (CMO) using a CMO labeling for Single Cell RNA Sequencing Protocol from 10x Genomics. Cells labeled with CMOs were washed, labelled with SytoxGreen and Hoescht to ensure cell viability and live cells sorted with a FACs Aria cell sorter. Samples were pooled and single-cell RNA-seq was performed following the Chromiun Next GEM Single Cell 3' v3.1 with feature barcode technology for cell multiplexing protocol (10x Genomics). Briefly, cells were first counted and checked their viability using Countess 3 cell counter (Thermofisher). Next, cells were loaded onto a 10x Genomics chip of the Chromium Controller (10x Genomics). After cDNA amplification, gene expression and CMO libraries were generated and sequenced using an Single-cell. Each sample was labeled with a cell multiplexing oligo (CMO) using a CMO labeling for Single Cell RNA Sequencing Protocol from 10x Genomics. Cells labeled with CMOs were washed, labelled with SytoxGreen and Hoescht to ensure cell viability and live cells sorted with a FACs Aria cell sorter. Samples were pooled and single-cell RNA-seq was performed following the Chromiun Next GEM Single Cell 3' v3.1 with feature barcode technology for cell multiplexing protocol (10x Genomics). Briefly, cells were first counted and checked their viability using Countess 3 cell counter (Thermofisher). Next, cells were loaded onto a 10x Genomics chip of the Chromium Controller (10x Genomics). After cDNA amplification, gene expression and CMO libraries were generated and sequenced using an Illumina NextSeq 2000 sequencer.

Raw sequencing data processing was performed from FASTQ file from each port using Cell Ranger (v6.1.2) with default parameters and the mm10 (GRCm38.p6) mouse genome reference provided by 10x Genomics. Obtained raw unique molecular identifier (UMI) count matrices of valid barcoded cells for each port were loaded into R (v4.1.2) for further analyses using Bioconductor packages (Amezquita RA, et al. Orchestrating single-cell analysis with Bioconductor. Nat Methods. 2020 Feb;17(2):137-145. doi: 10.1038/s41592-019-0654-x) and Seurat (v4.0.6) (Hao Y, et al. Integrated analysis of multimodal single-cell data. Cell. 2021 Jun 24;184(13):3573-3587.e29).

scRNA-seq preprocessing and main analyses were performed from obtained raw UMI count matrix for each port. Cells were filtered according to the total number of UMI counts (≥ 1,000 and ≤ 50,000), total number of detected genes (≥ 200 and ≤ 6,000), and % of mitochondrial UMI counts (≥ 7.5 %). Then, resulted cells were demultiplexed using the cellhashR R package (v1.0.2) (Boggy GJ, et al. BFF and cellhashR: analysis tools for

accurate demultiplexing of cell hashing data. Bioinformatics. 2022 May 13;38(10):2791-2801) using htodemux, bff_cluster, gmm_demux, multiseq, and dropletutils methods. Consensus classification was used for further analyses. Once the final set of cells was obtained, transcriptional expression values were normalized to total UMI counts per cell multiplied by a scaling factor of 10,000 and natural-log transformed (NormalizeData function). Highly variable genes were defined using VST method as implemented in Seurat setting a total of 2,000 highly variable genes, and PCA was used to reduce this dimensional space after scaling log-transformed expression values. In this step, unwanted sources of variability (total number of counts) were regressed out using the ScaleData function with a linear model. Elbow plot method was used to determine the number of PCs for downstream analyses (25 PCs). Then, cells were clustered using the Louvain algorithm for modularity optimization using KNN graph as input and visualized using the Uniform Manifold Approximation and Projection for Dimension Reduction (UMAP) algorithm with the first 25 principal components as input. Main clusters were identified by using known markers and calculating differentially expressed genes with Wilcoxon-rank sum test using presto R package (v1.0.0); Extended Data Fig.4). Cell proportions were calculated for each condition and time point in every cell population, and a two-proportions Z-test using the prop.test R function was chosen to determine significance.

Differential expression analyses between conditions were independently performed on every cell population comparing ImP vs control for each timepoint using the MAST R package (v1.20.0). Genes were ranked according to the calculated logFCs, and resulting ranks were used as input for the FGSEA algorithm along with the Hallmark gene sets from the Molecular Signature Data Base (MSigDB; https://www.gsea-msigdb.org/gsea/msigdb). In order to identify specific cell subpopulations for every general cell type, each population was separated and independently analyzed using the same workflow explained above. Subclusters were identified by using known markers and calculating differentially expressed genes with the presto R package. Finally, overrepresentation analysis considering gene markers for every identified subcluster was performed along with the GO database (www.geneontology.org/) in order to interpret the transcriptional state of each subpopulation.

Based on unsupervised graph-based clustering algorithm and manual annotation by classical markers seven clusters were defined according to their gene expression profiles (Fig 4c), highlighting a significant decrease in the proportions of vascular smooth cells

and a significant increase in fibroblasts (FBs), endothelial cells (ECs) and immune cells populations, particularly after 8 weeks of ImP supplementation (Fig. 4d). Moreover, focusing on the immune cell compartment, at 8 weeks, a remarkable enrichment of T cells (logFC: +3.12, C vs ImP, P<0.00001) and B cells (logFC: +4.61, C vs ImP, P<0.00001) in the aorta of *ApoE*$^{-/-}$ fed chow diet when treated with ImP, which was also confirmed by FACS (Fig. 4e), suggesting a link between ImP treatment and an adaptive immune response. When considering the effects of ImP on aortic cells at a very early stage of plaque development (4weeks), scRNAseq data showed a similar trend towards enriched FBs, MFs and ECs proportions after 4 weeks on ImP treatment, suggesting that the effects of ImP can be detected also at this earlier time point. To further explore the transcriptional changes that are associated with ImP-driven atherosclerosis, the cell populations (i.e. ECs, MFs and FBs) that were increased upon the treatment were examined. A gene set enrichment analysis for each cluster was performed by comparing cells from mice treated or not with ImP, pointing out an increased expression of genes related to inflammation, in particular to the *TNFα* signaling via the *NFKB* pathway, being associated with ImP treatment in all cell types (Fig. 4f).

Example 5: mTOR activation in immune cells contributes to ImP-induced inflammatory response and atherosclerosis.

In line with previous data, we analyzed the direct effect of ImP in vitro in several cell types. Mouse embryonic fibroblast (MEF) cell lines were isolated from 13.5 dpc from embryos using standard protocol. Each embryo was dissected into 10ml of sterile PBS, voided of its internal organs, head, and legs. After 30 min incubation with gentle shaking at 37°C with 5ml 0,1% trypsin, cells were plated in two 100 mm dishes and incubated for 24-48h. Mouse aortic endothelial cells (MAECs) were isolated from mouse thoracic aortas as described previously (REF). The cells were cultured (Medium 199 (Gibco, Invitrogen Life Technologies) + 20% fetal bovine serum + Penicillin/Streptomycin 2 mM + Glutamine 2 mM + HEPES 10 mM + endothelial cell growth supplement 30 lg/mL + Heparin 100 mg/mL, all from Sigma–Aldrich, under 5% CO_2 at 37C. Murine BMDMs were generated as previously described[13] with some modifications. BM cells from WT C57BL/6J mice were cultured in RPMI 1640 supplemented with 30% M-CSF obtained from L929 cell line and 10% FBS, 100 μg ml^{-1} penicillin, 100 μg ml^{-1} streptomycin, 10 mM HEPES, 1 nM sodium pyruvate (all from Gibco) during 5 days in sterile, but not tissue-culture treated, 10-cm Petri dishes.

Cultured MEF, MAECs and BMDM were plated in equal number ($1x10^5$ cells per well) in 96-well plates (200-µl final volume, Corning) and rested overnight. Cells were treated in vitro with ImP, 10µg/mL or not (Ctrol) co-incubated with Rapamycin (10nM). After 24h supernatant was collected and TNFα concentration was quantified with Mouse TNF-alpha DuoSet ELISA (DY410) according to manufacture instructions (Fig 5a). Cells were collected and labelled with Phospho-S6-PE (Cell Signalling #5316) according to the manufacture protocol, activation was measured by flow cytometry MFI (Fig 5b). To assess the key role of mTOR pathway in the ImP induce AT, $LDLr^{-/-}$ mice were irradiated with 2 doses of 5.5Gy and grafted with bone marrow collected from mice impaired in mTORC1 in macrophages (LysMcre-Raptor mice). After 30 days grafted mice were treated with ImP as was described (Fig 5c). The selective depletion of mTOR1 in MFs was able to prevent the development of AT induce by ImP (Fig 5d). These findings support an ImP-dependent activation of mTOR pathway in MFs has a detrimental role in atherosclerosis.

Example 6: ImP mediates its effect on atherosclerosis through the imidazoline receptor 1

To experimentally confirm the possible link between ImP and imidazoline receptors (IRs) I1 and I2, BMDM and MEF were stimulated with ImP in the presence of AGN192403 (10 µg/mL, I1R ligand with antagonist functions), idazoxan (0.06 µg/mL, IR antagonist with high affinity for I2R), or yohimbine (1 µg/mL, a potent α2-adrenoceptor antagonist with low affinity for IRs). In all cell lines, it was found that the ability of ImP to increase the phosphorylation of S6 and to induce TNFα were prevented when preincubated with AGN192403 (Fig. 6 a,b), but not with the other antagonists tested, pointing out ImP as a selective I1R endogenous ligand.

To determine whether the blockade of this axis halts the ImP atheroprone effects, chow-fed *ApoE*$^{-/-}$ mice were treated with ImP (400ug/mL) and AGN192403 (30ug/mL) in the drinking water for 8 weeks. It is shown that AGN192403 treatment prevented the formation of the ImP-induced atheroma plaque, independently of the bloodstream concentration of total cholesterol and LDL-C (Fig. 7a,b), suggesting that the effect of ImP on atherosclerosis and thus of its antagonist might be independent of lipid accumulation.

In line with this, the AGN192403 treatment dampened the systemic inflammation and the adaptive response induced by ImP, specifically by reducing the expansion of $Ly6C^{hi}$ monocytes and Th1 cells. The concentration of pro-inflammatory cytokines, INFγ and

TNFa was measure in the serum according manufactures protocol using Mouse IFN-gamma DuoSet ELISA (DY485), respectably and Mouse TNF-alpha DuoSet ELISA (DY410). INFγ and TNFα were found normalized by AGN192403. Besides, AGN192403 treatment inhibited the activation of the mTOR pathway in peritoneal macrophages (Fig. 7e). The aorta was collected as was describe before to analyze the immune cells infiltrated, the AGN192403 treatment blocked the ability of ImP to induce a Th1/Treg polarization (Fig. 7f) by increasing the Treg population and decreasing Th1 cell infiltration (Extended Fig. 7g).

Example 7: Inhibition of the I1R/ImP pathway prevents atherosclerosis progression

To further assess the capacity of the blockade of the ImP/I1R axis to treat atherosclerosis, the disease was induced by feeding *ApoE*$^{-/-}$ mice with HC diet for 8 weeks, thereby increasing the ImP production (Fig. 1g). Mice were supplemented with AGN192403 during the last 4 weeks on diet. It resulted in a reduction in the atheroma plaque in the treated mice (Fig. 8a) without effect on total cholesterol or LDL-C (Fig. 8b) alongside a systemic reduction in Ly6C^{hi} monocytes (Fig. 8c) as well as a normalization of Th1 cells numbers in blood (Fig. 8d) and pro-inflammatory cytokine concentration IFNγ measured (Fig. 8e) Moreover, the treatment reduced the activation of mTOR in peritoneal macrophages (Fig. 8f). Notably, this protective effect occurred despite the increased cholesterol levels in the bloodstream of HC-fed mice.

Claims

1. An antagonist of imidazoline-1 receptor (I1R), or a pharmaceutically acceptable salt, tautomer, solvate, diastereomer, enantiomer, or prodrug thereof, as valence and stability permit, for use in the prevention and/or treatment of an autoinflammatory or autoimmune disease in a human subject,

   in which said antagonist of I1R is selected from the group consisting of
   (±)-2-endo-amino-3-exo-isopropylbicyclo[2.2.1]heptane,
   N-benzylguanidine,
   2-(2-Fluoro-5-methylphenyl)-4,5-dihydro-1H-imidazole,
   2-(2-chloro-4-iodo-phenylamino)-5-methyl-pyrroline,
   1-(4, 5-dihydro-1H-imidazol-2-yl)isoquinoline,
   5-[2-bromophenoxy)methyl]-4,5-dihydro-1,3-oxazol-2-amine,
   6-methylamino-2methylheptene, and
   4-chloro-2,3-dihydro-2-oxo-1,3-benzothiazol-3-ylacetic acid.

2. An antagonist of I1R for use according to claim 1, in which said antagonist of I1R is (±)-2-endo-amino-3-exo-isopropylbicyclo[2.2.1]heptane.

3. An antagonist of I1R for use according to claim 1 or 2, in which said salt is the hydrochloride salt.

4. An antagonist of I1R for use according to any one of claims 1 to 3, in which said human subject has a level of ImP in blood of at least 41nM.

5. An antagonist of I1R for use according to any one of claims 1 to 4, in which said autoinflammatory or autoimmune disease is atherosclerosis.

6. A pharmaceutical composition comprising an antagonist I1R for use according to any one of claims 1 to 5, and at least one pharmaceutically suitable excipient.

7. Method for screening and/or producing therapeutic candidates for the prevention and/or treatment of an autoinflammatory or autoimmune disease, comprising in-vitro assessing whether a therapeutic candidate is able to inhibit the binding of ImP to I1R, wherein a positive result indicates that the therapeutic candidate is defined by this assay as a I1R antagonist and useful for the treatment of said autoinflammatory or autoimmune disease.

8. Use of Imidazole propionate (ImP) in the diagnosis of an autoinflammatory or autoimmune disease in a biological sample obtained from a subject.

9. Use according to claim 8, in which said biological sample is a blood sample.

10. Use according to claim 9, in which said blood sample is a plasma sample.

11. Use according to any one of claims 8 to 10, in which said autoinflammatory or autoimmune disease is atherosclerosis.

12. Use according to any one of claims 8 to 11, in combination with an additional marker of atherosclerosis.

13. A method of diagnosis of atherosclerosis, comprising:

- assessing the level of ImP in a blood sample obtained from a human subject, and

- determining whether said level is above or below a value of 41nM, wherein a value above 41nM is indicative of likelihood of having early atherosclerosis.

Figure 1

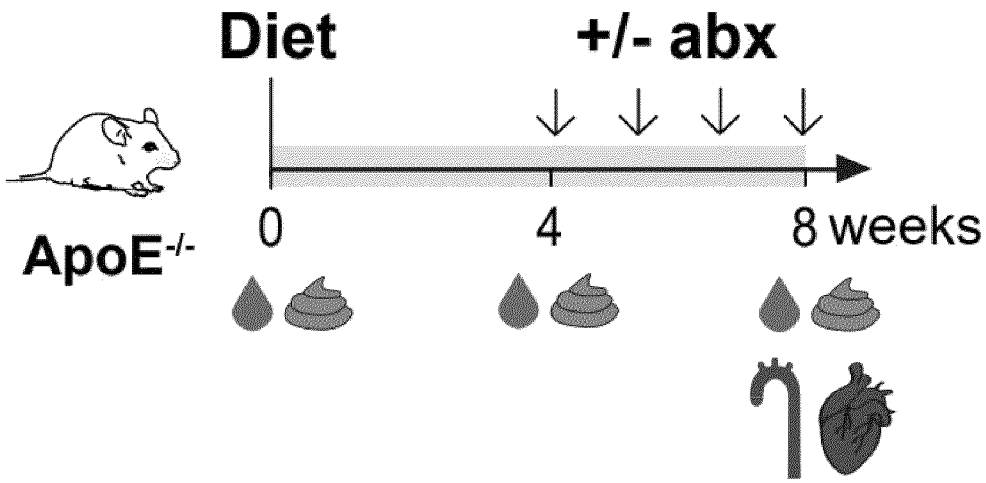

Figure 1a

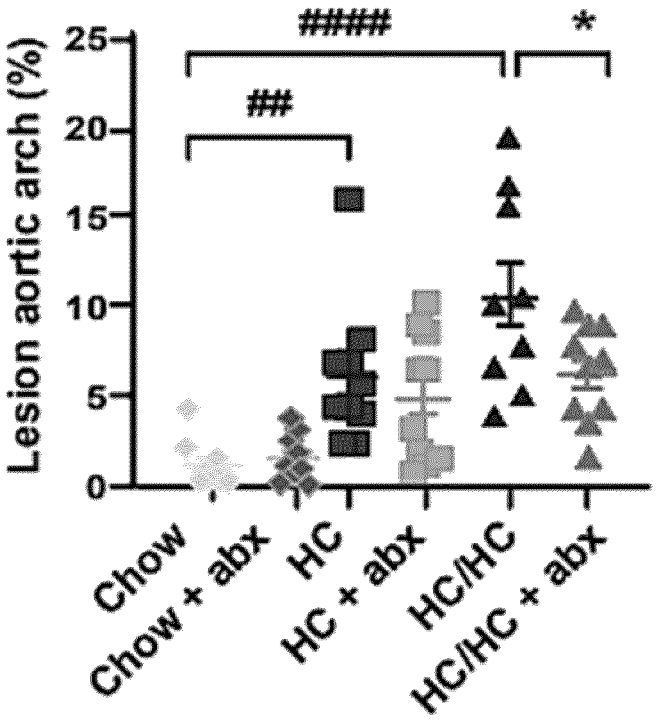

Figure 1b

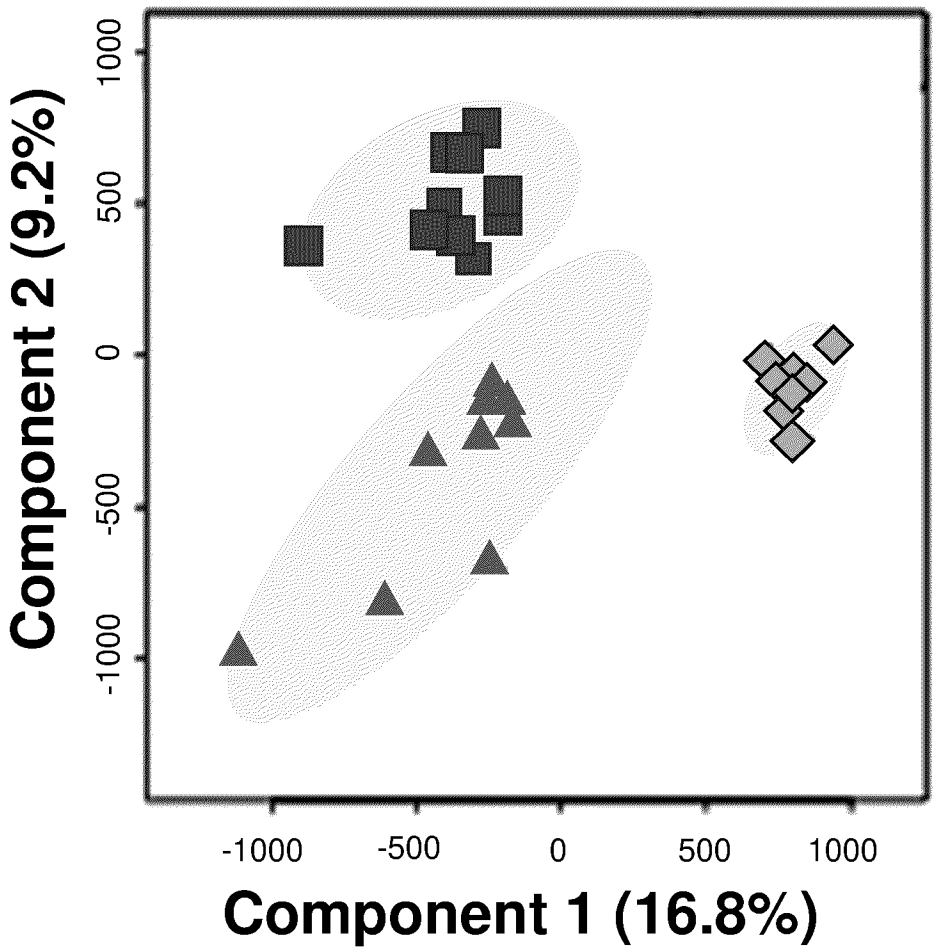
Component 2 (9.2%)
1000
500
0
-500
-1000
-1000
-500
0
500
1000
Component 1 (16.8%)

Figure 1c

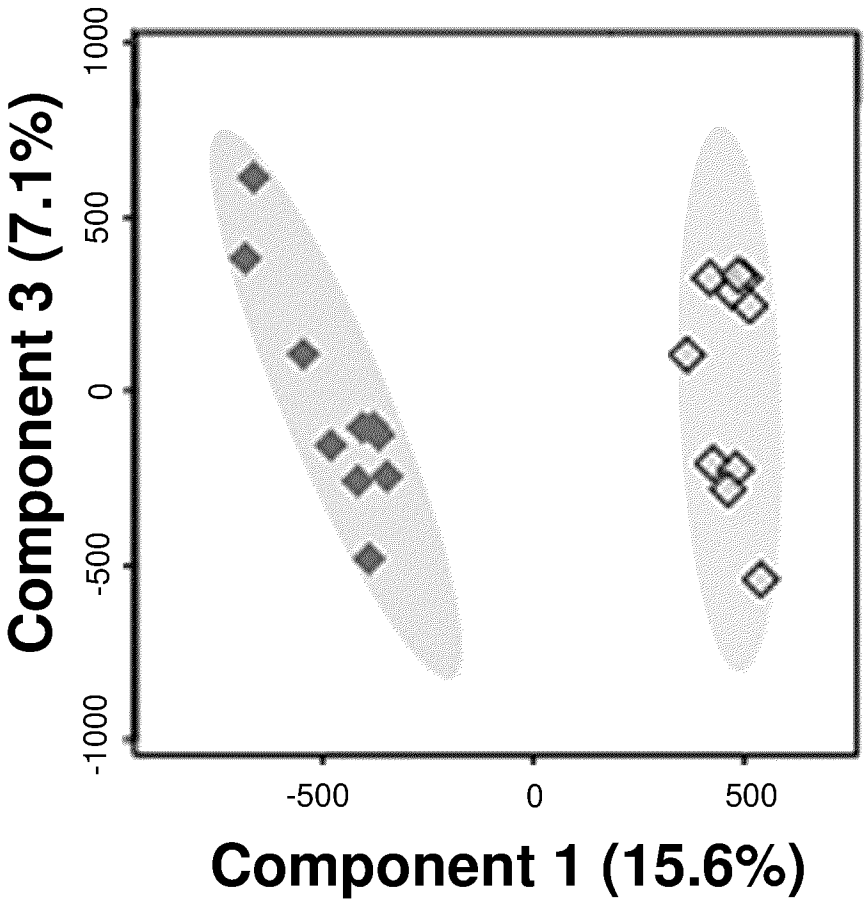

Figure 1d

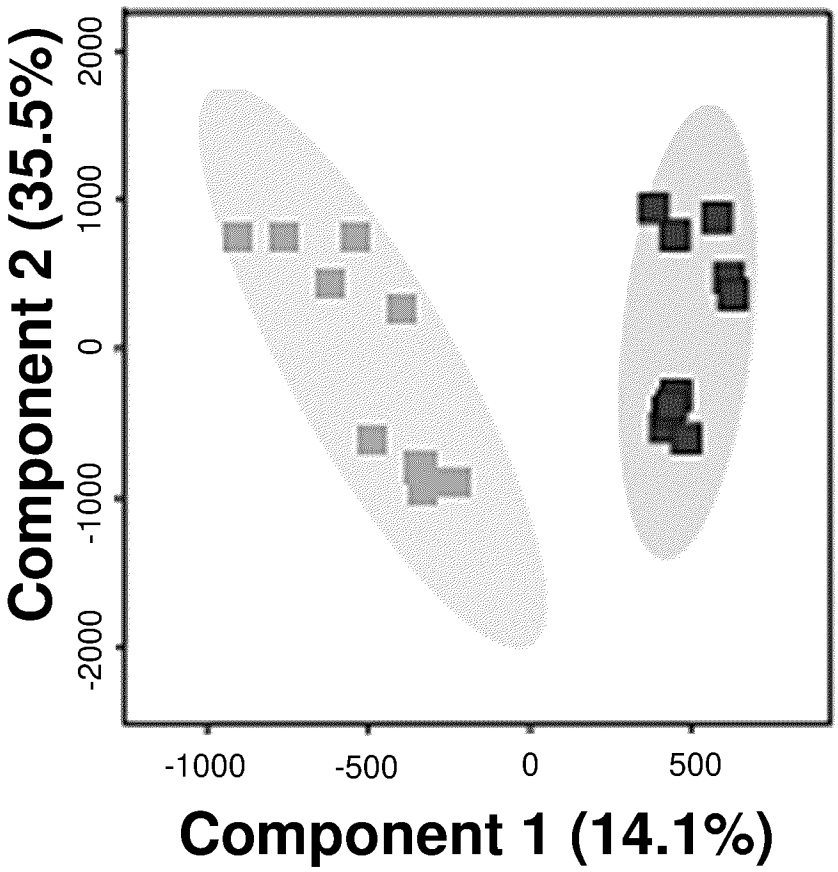
Component 2 (35.5%)
2000
1000
0
-1000
-2000
-1000
-500
0
500
Component 1 (14.1%)

Figure 1e

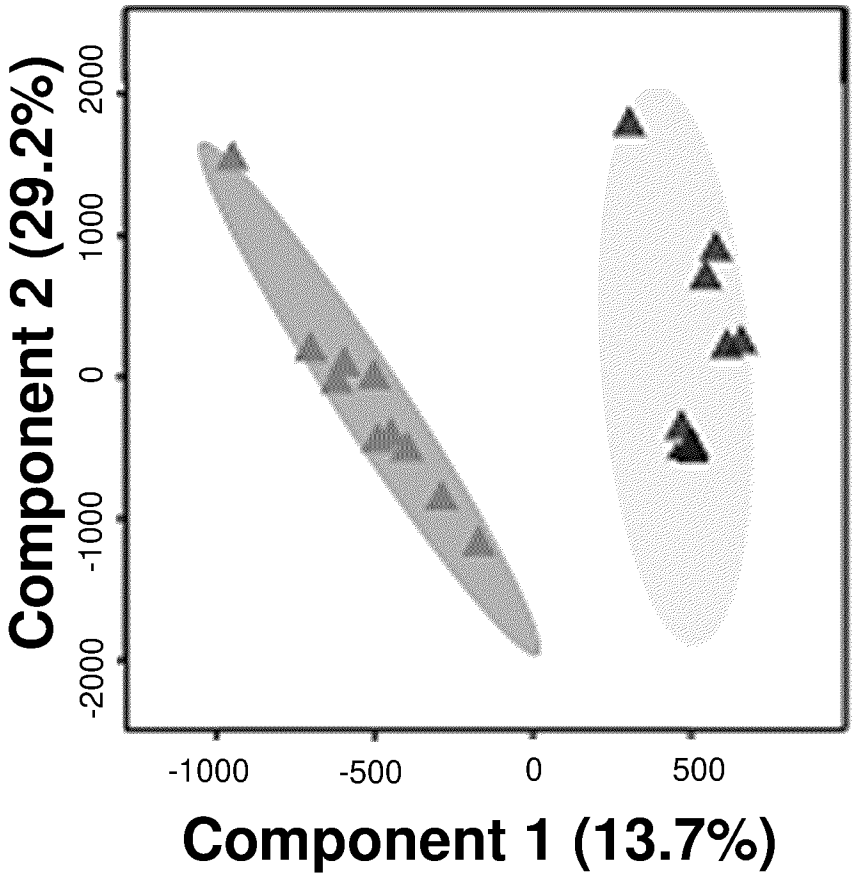
Component 2 (29.2%)
2000
1000
0
-1000
-2000
-1000
-500
0
500
Component 1 (13.7%)

Figure 1f

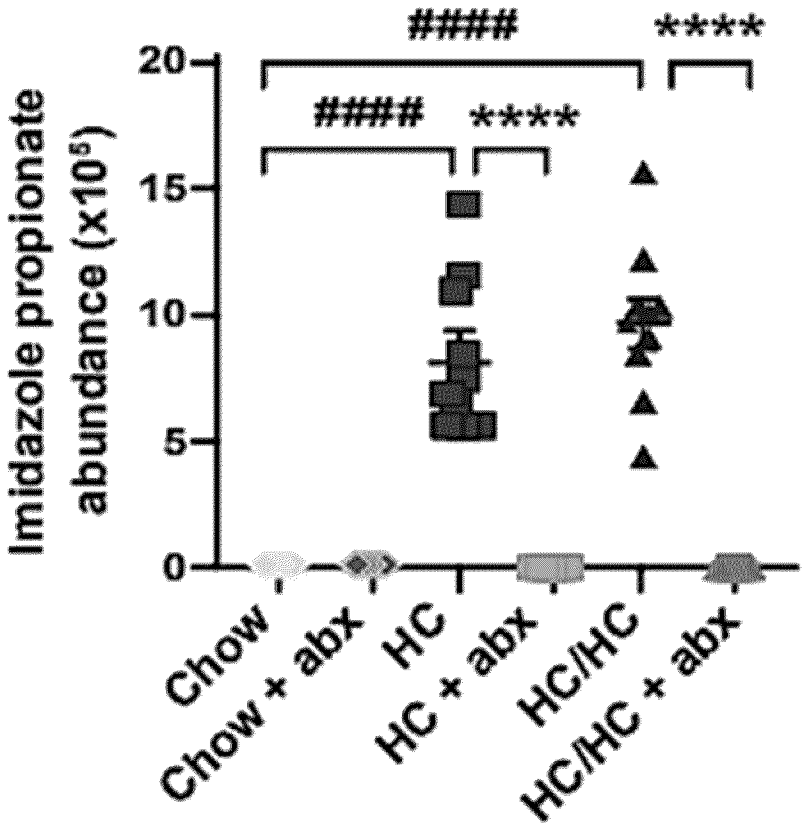

Figure 1g

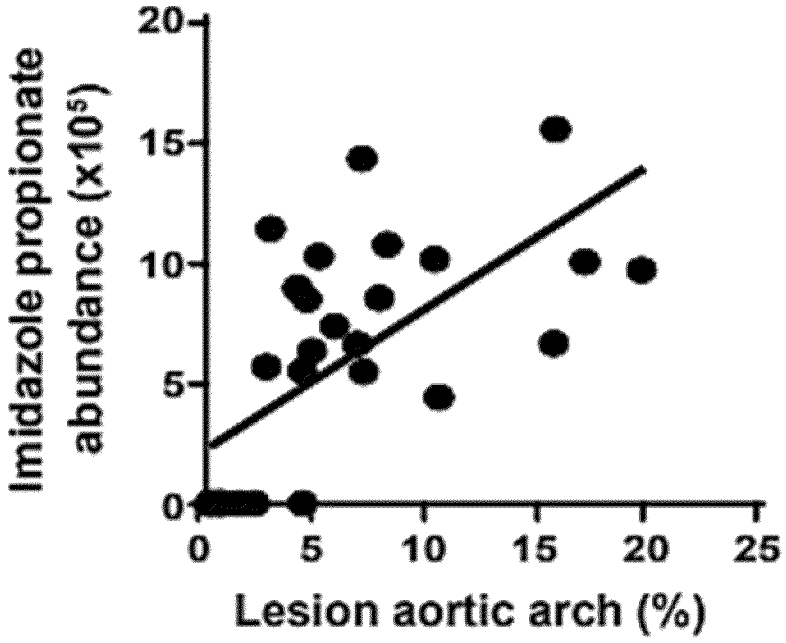

Figure 1h

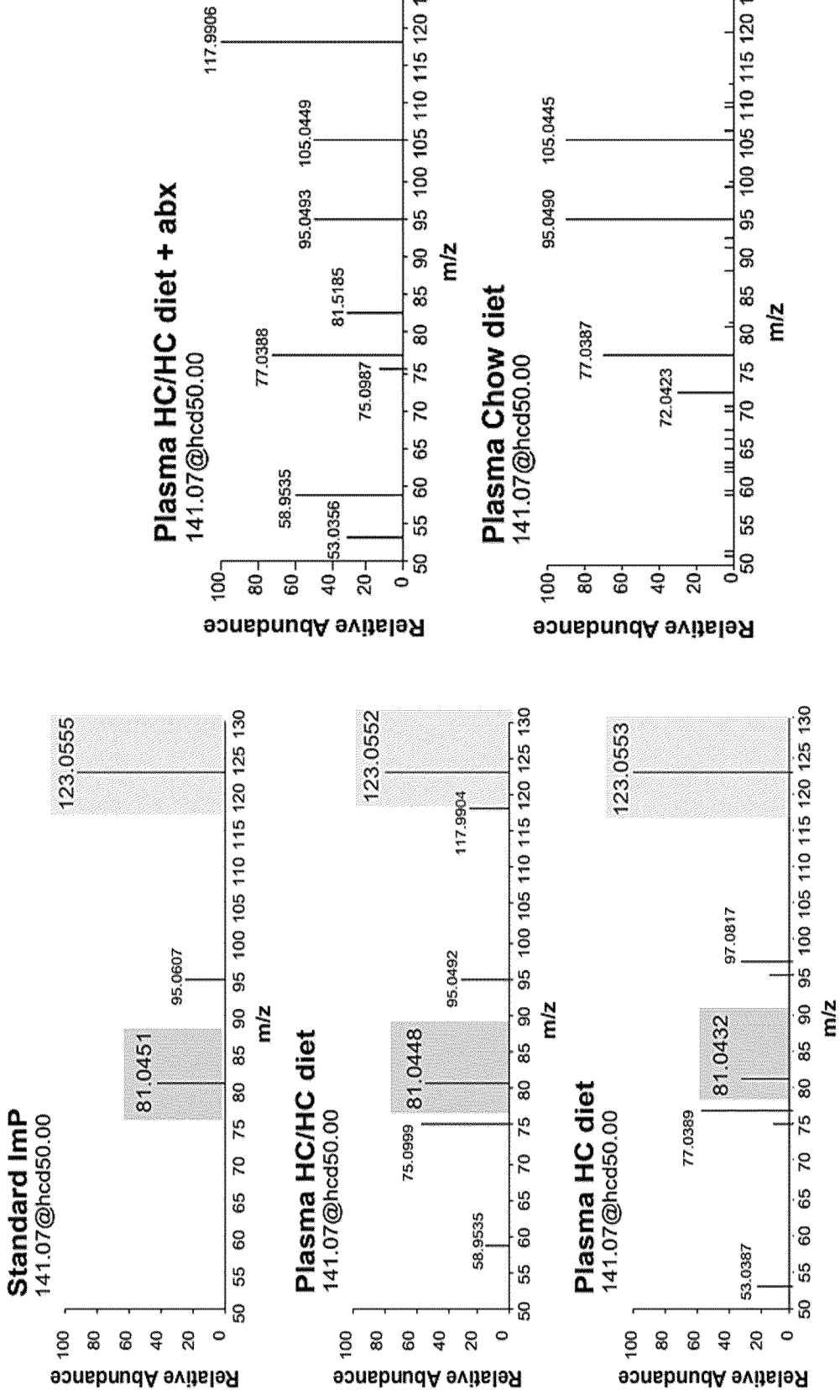
Standard ImP
141.07@hcd50.00
123.0555
81.0451
95.0607
Plasma HC/HC diet
141.07@hcd50.00
123.0552
75.0999
81.0448
95.0492
58.9535
117.9904
Plasma HC diet
141.07@hcd50.00
123.0553
77.0389
81.0432
97.0817
53.0387
Plasma HC/HC diet + abx
141.07@hcd50.00
117.9906
77.0388
58.9535
81.5185
95.0493
105.0449
53.0356
75.0987
Plasma Chow diet
141.07@hcd50.00
95.0490
105.0445
77.0387
72.0423
Relative Abundance
m/z

Figure 1i

Figure 2

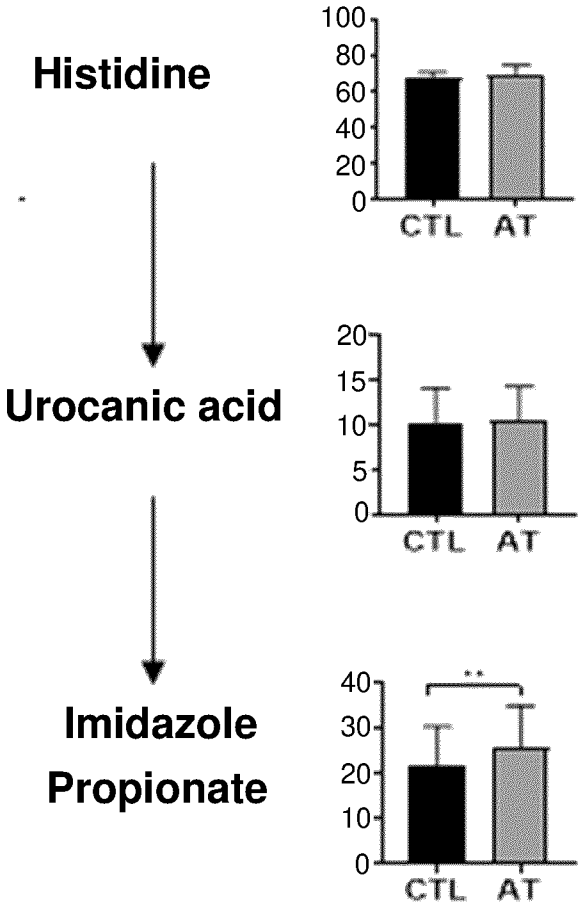

Figure 2a

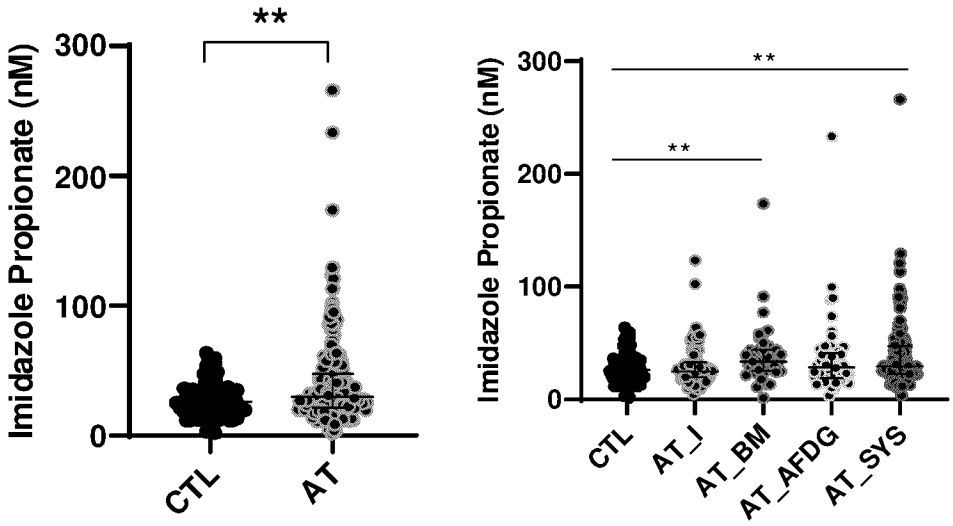

Figure 2b

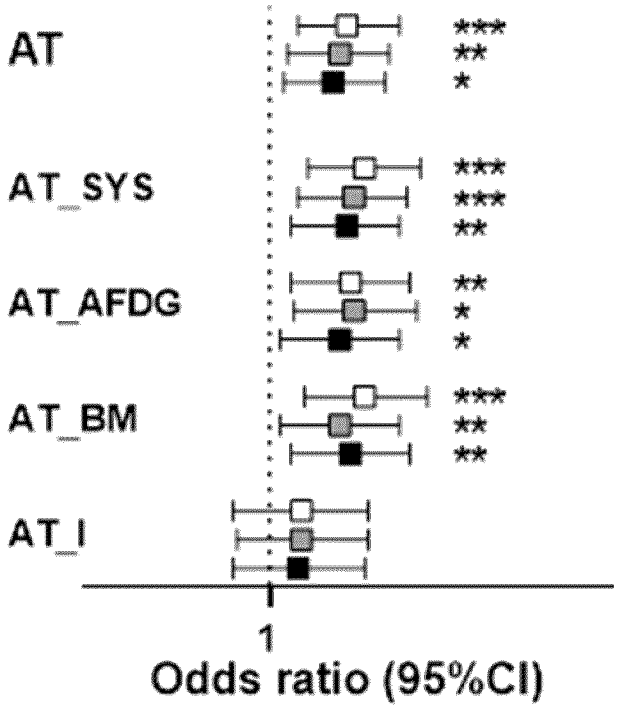

Figure 2c

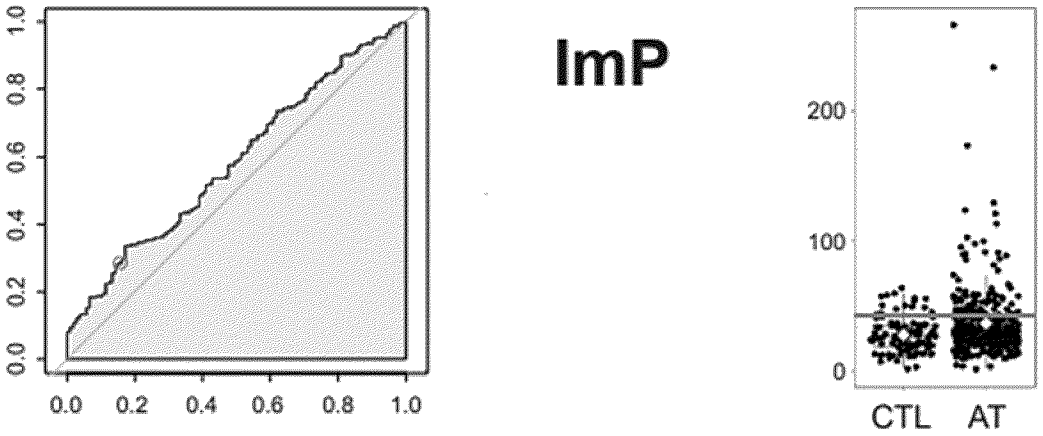

Figure 2d

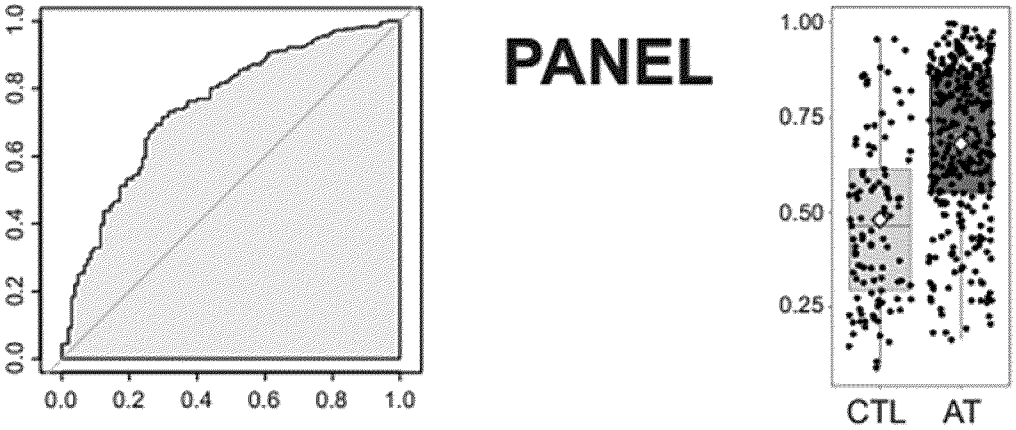

Figure 2e

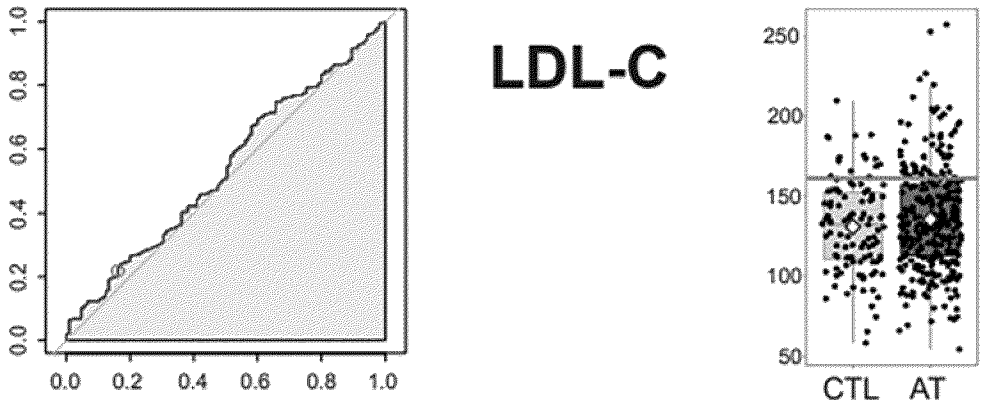

Figure 2f

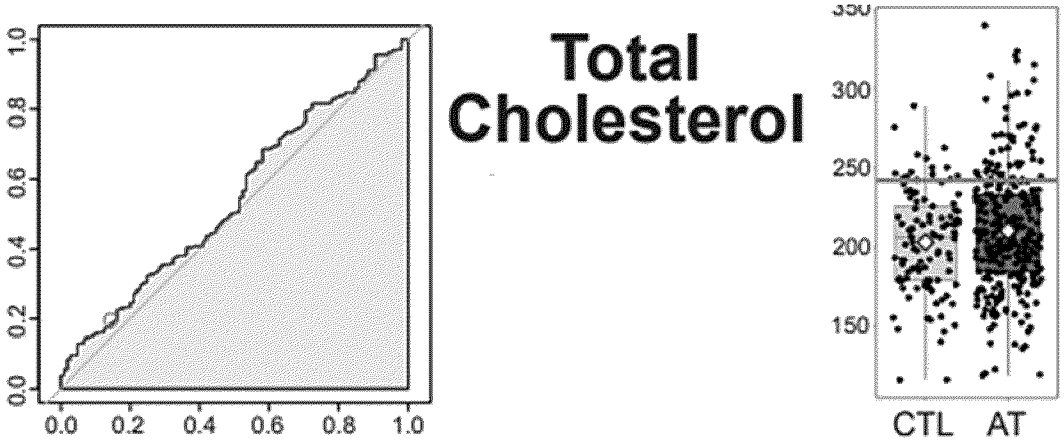

Figure 2g

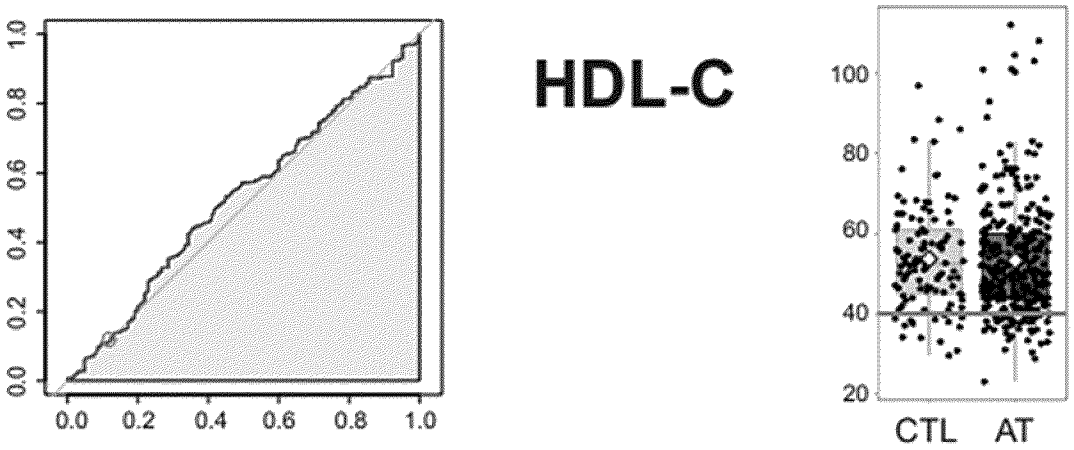

Figure 2h

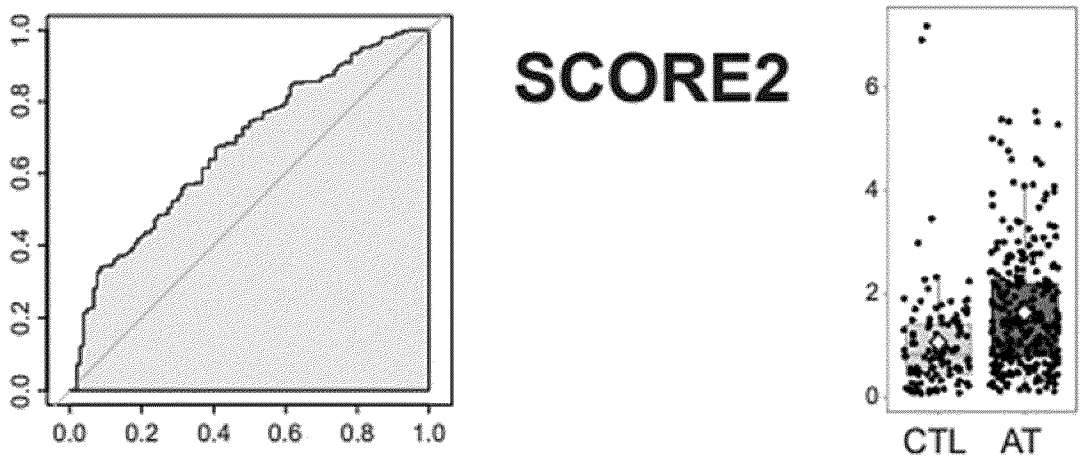

Figure 2i

Figure 3

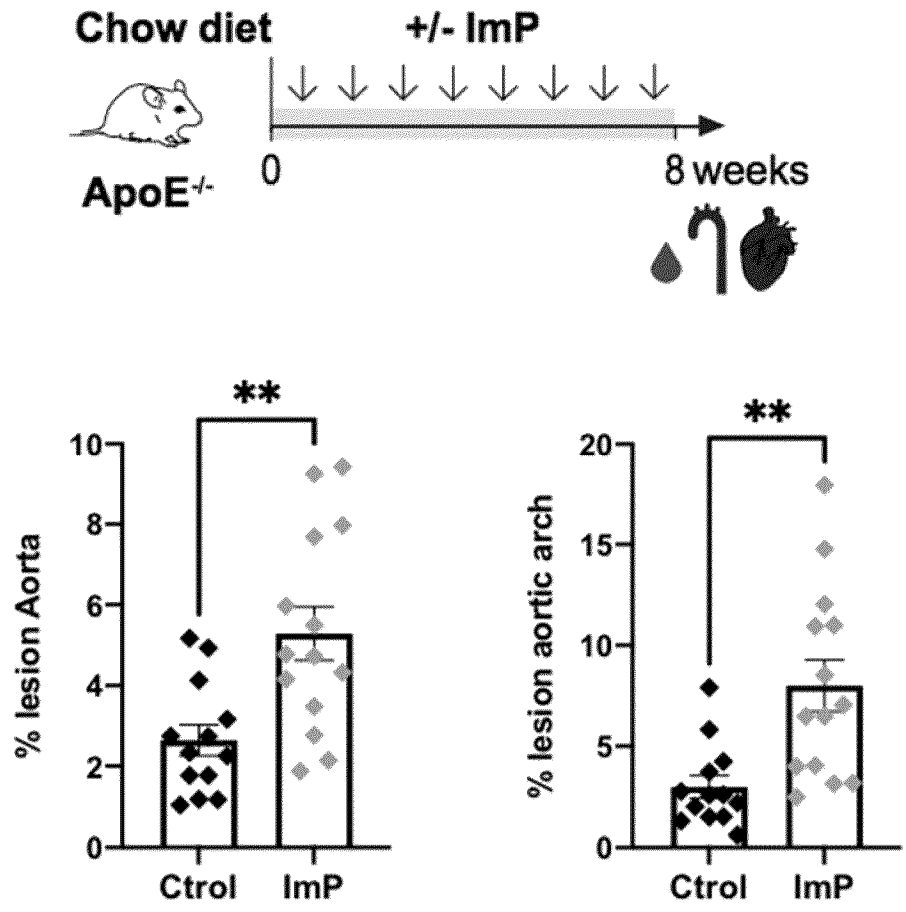

Figure 3a

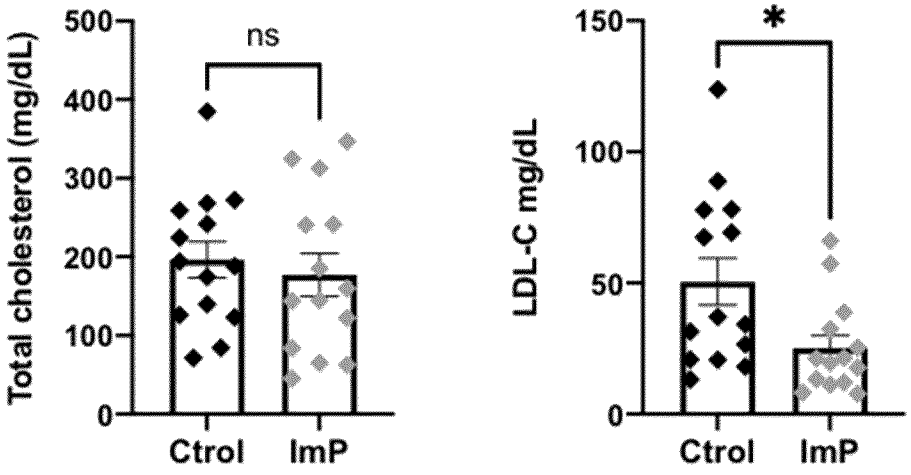

Figure 3b

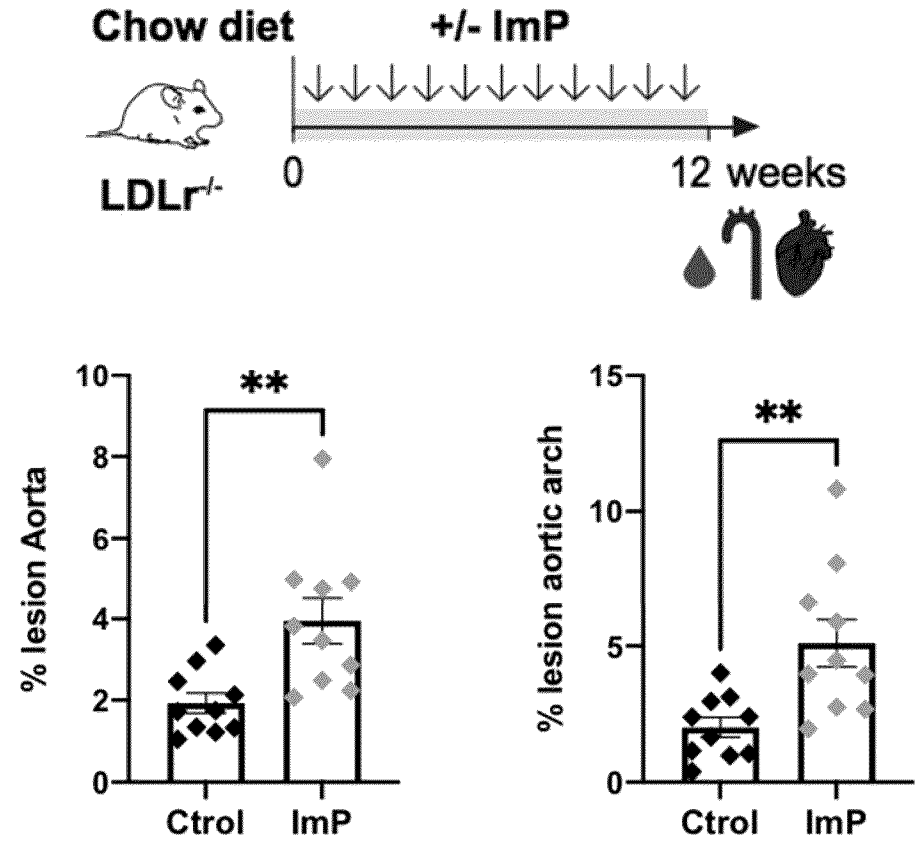

Figure 3c

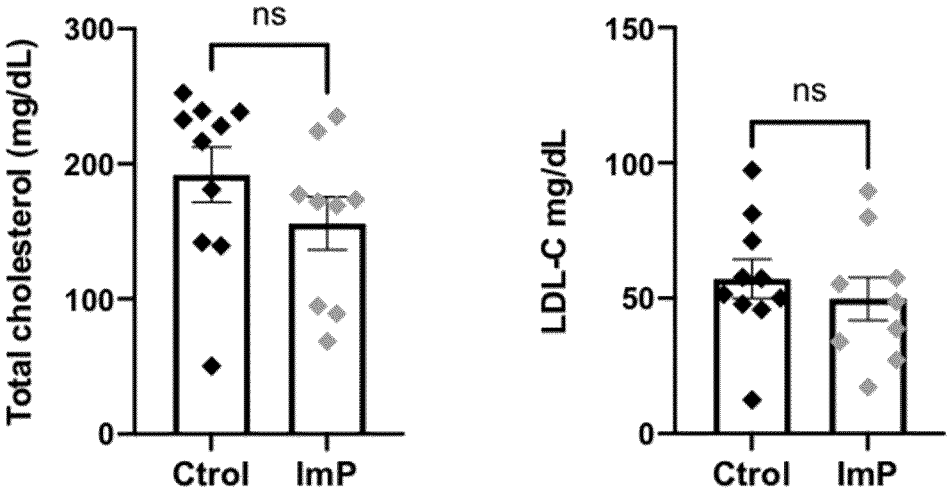

Figure 3d

Figure 4

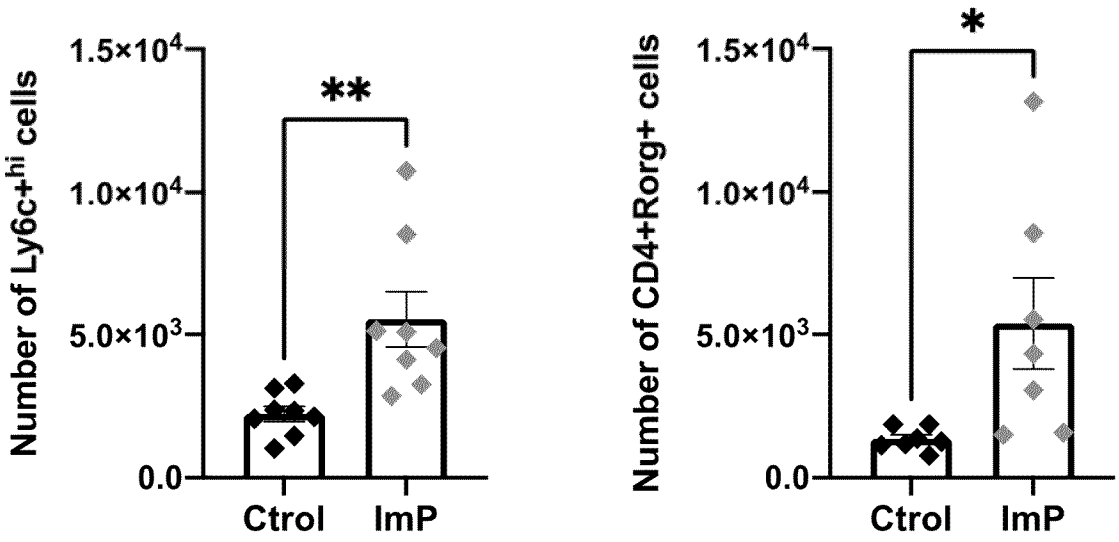

Figure 4a

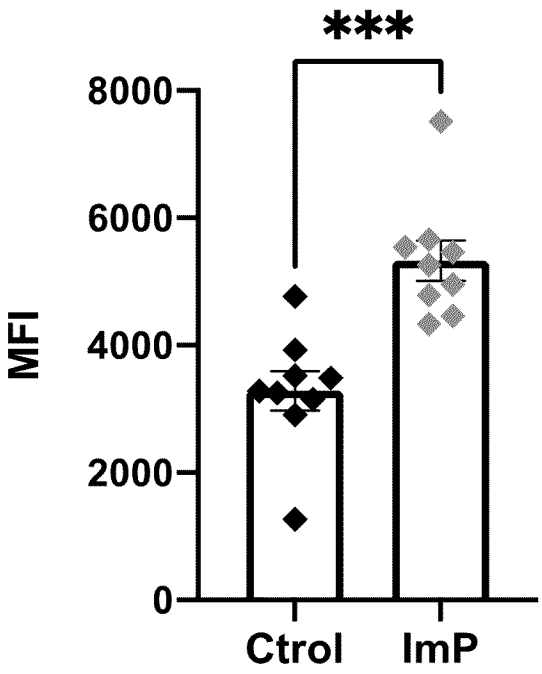

Figure 4b

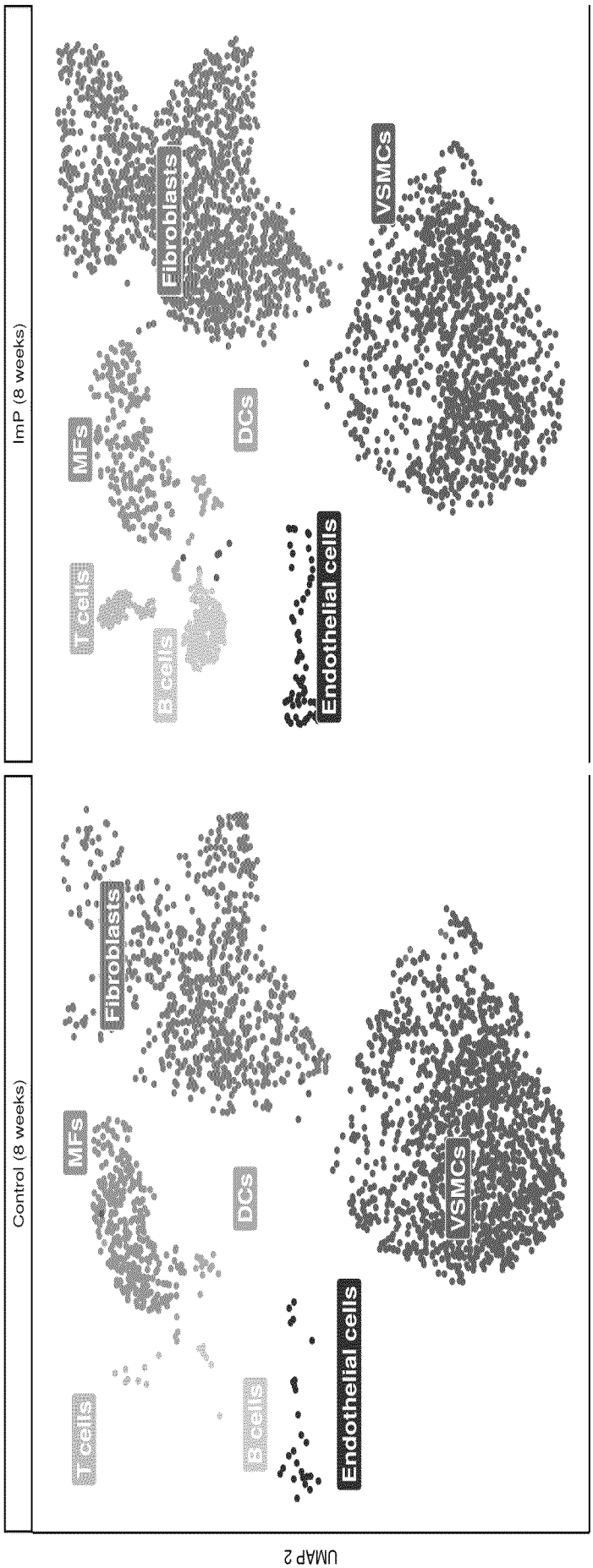
ImP (8 weeks)
Control (8 weeks)
Fibroblasts
MFs
T cells
B cells
DCs
Endothelial cells
VSMCs
UMAP 1
UMAP 2

Figure 4c

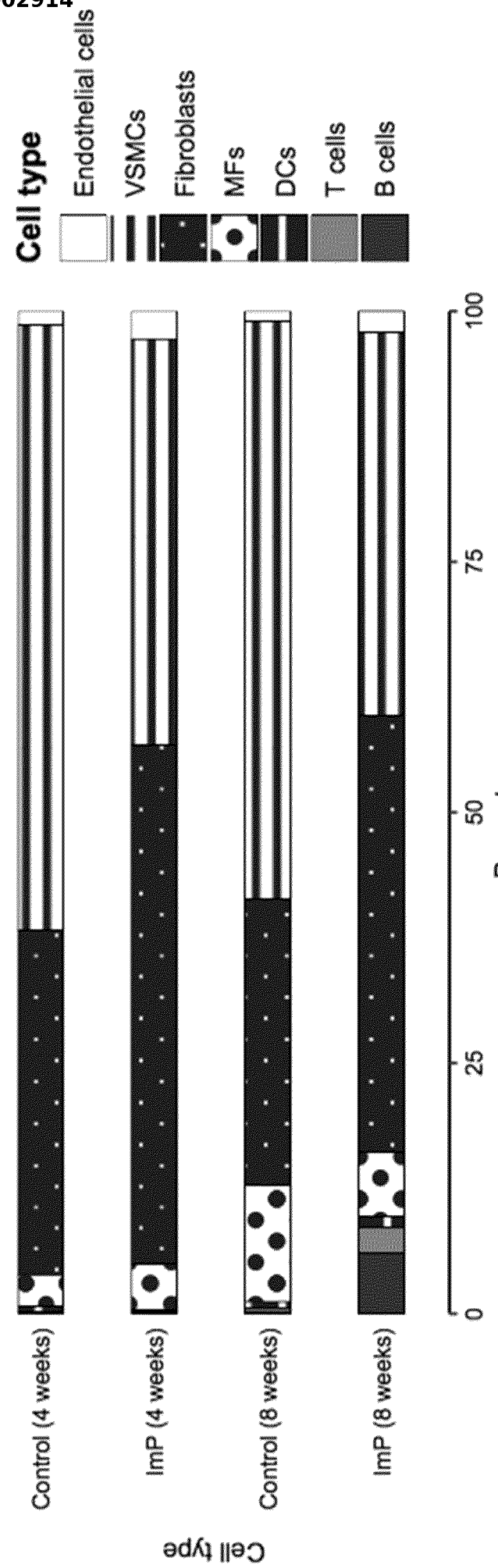
Cell type
Endothelial cells
VSMCs
Fibroblasts
MFs
DCs
T cells
B cells
Control (4 weeks)
ImP (4 weeks)
Control (8 weeks)
ImP (8 weeks)
Cell type
0
25
50
75
100
Percentage

Figure 4d

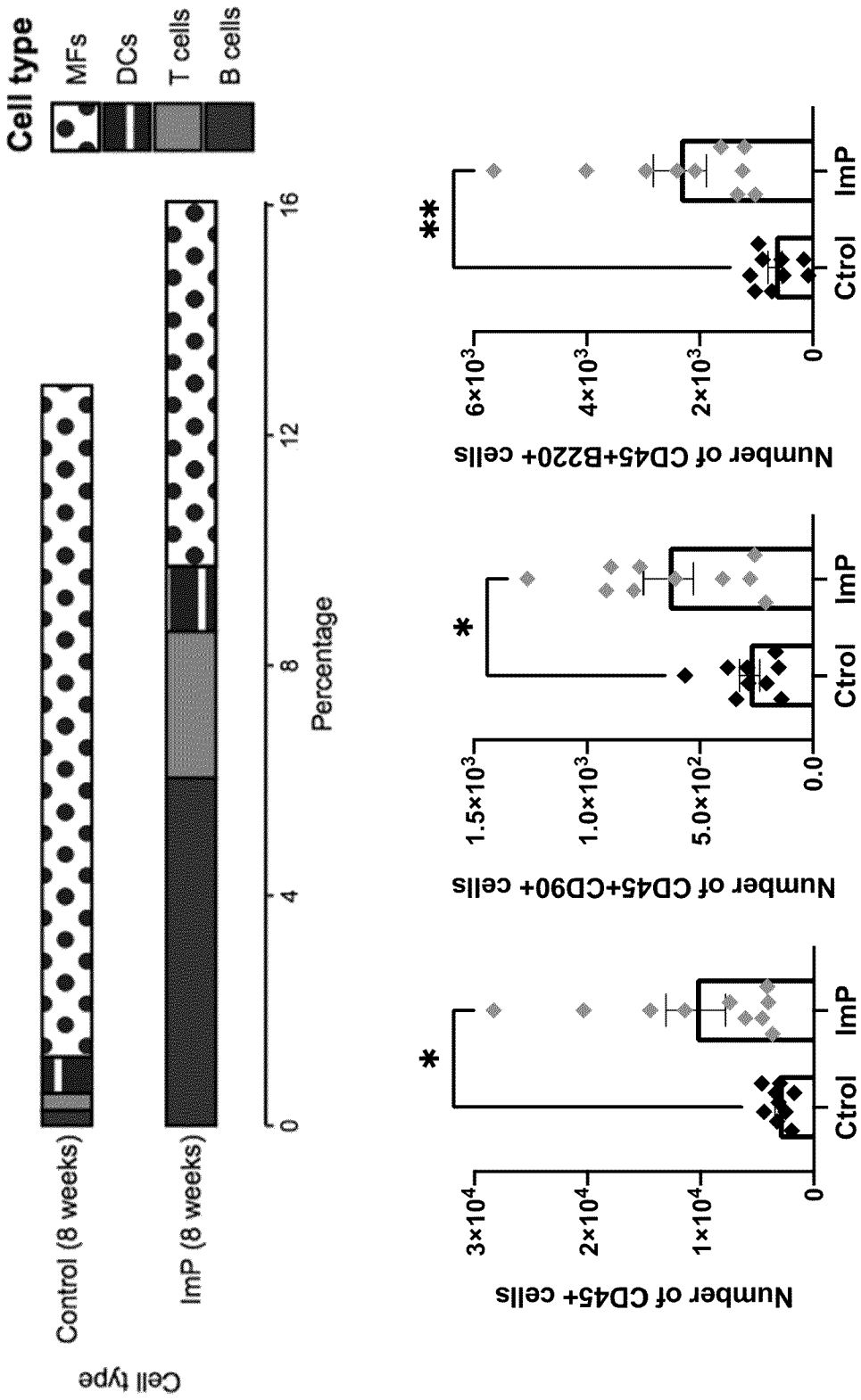
Cell type
MFs
DCs
T cells
B cells
Control (8 weeks)
ImP (8 weeks)
Cell type
0
4
8
12
16
Percentage
Number of CD45+ cells
3×10^4
2×10^4
1×10^4
0
Ctrol
ImP
*
Number of CD45+CD90+ cells
1.5×10^3
1.0×10^3
5.0×10^2
0.0
Ctrol
ImP
*
Number of CD45+B220+ cells
6×10^3
4×10^3
2×10^3
0
Ctrol
ImP
**

Figure 4e

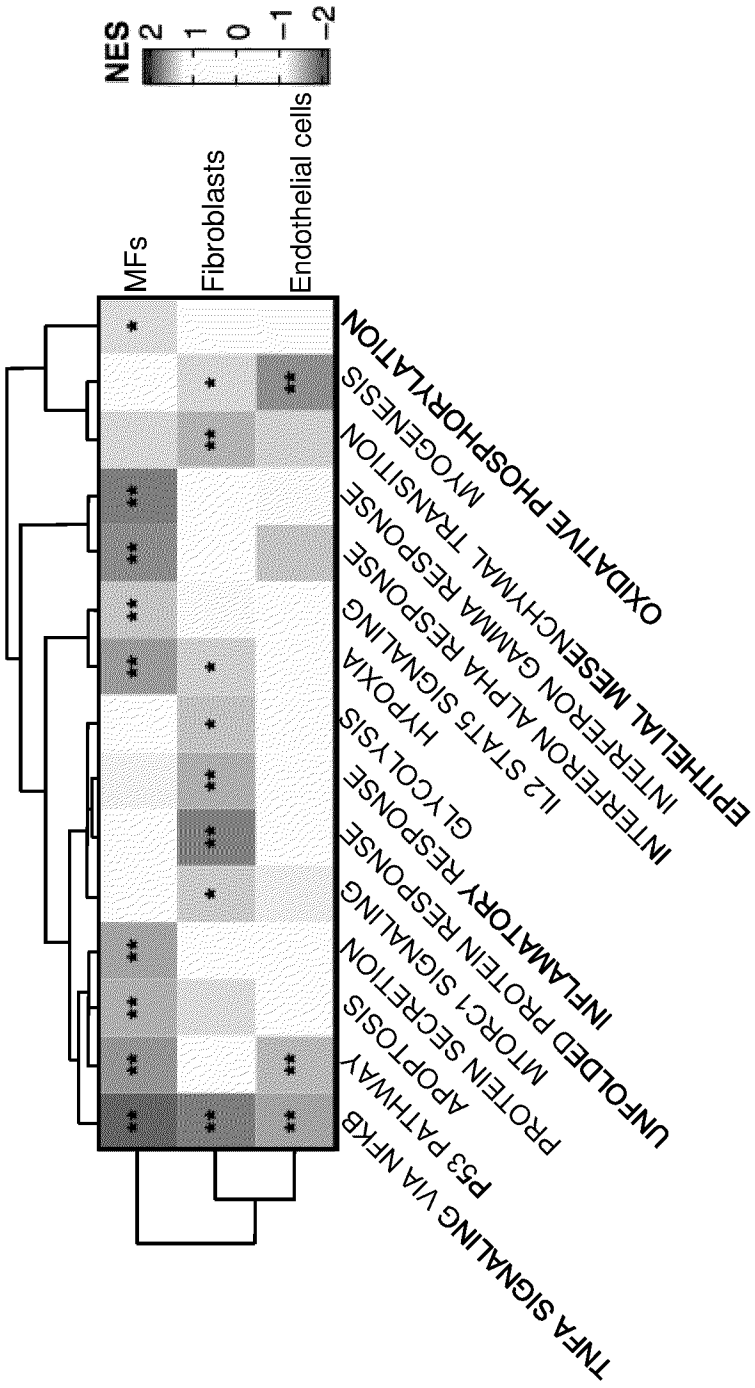
NES
2
1
0
−1
−2
MFs
Fibroblasts
Endothelial cells
TNFA SIGNALING VIA NFKB
P53 PATHWAY
APOPTOSIS
PROTEIN SECRETION
MTORC1 SIGNALING
UNFOLDED PROTEIN RESPONSE
INFLAMMATORY RESPONSE
GLYCOLYSIS
HYPOXIA
IL2 STAT5 SIGNALING
INTERFERON ALPHA RESPONSE
INTERFERON GAMMA RESPONSE
EPITHELIAL MESENCHYMAL TRANSITION
MYOGENESIS
OXIDATIVE PHOSPHORYLATION

Figure 4f

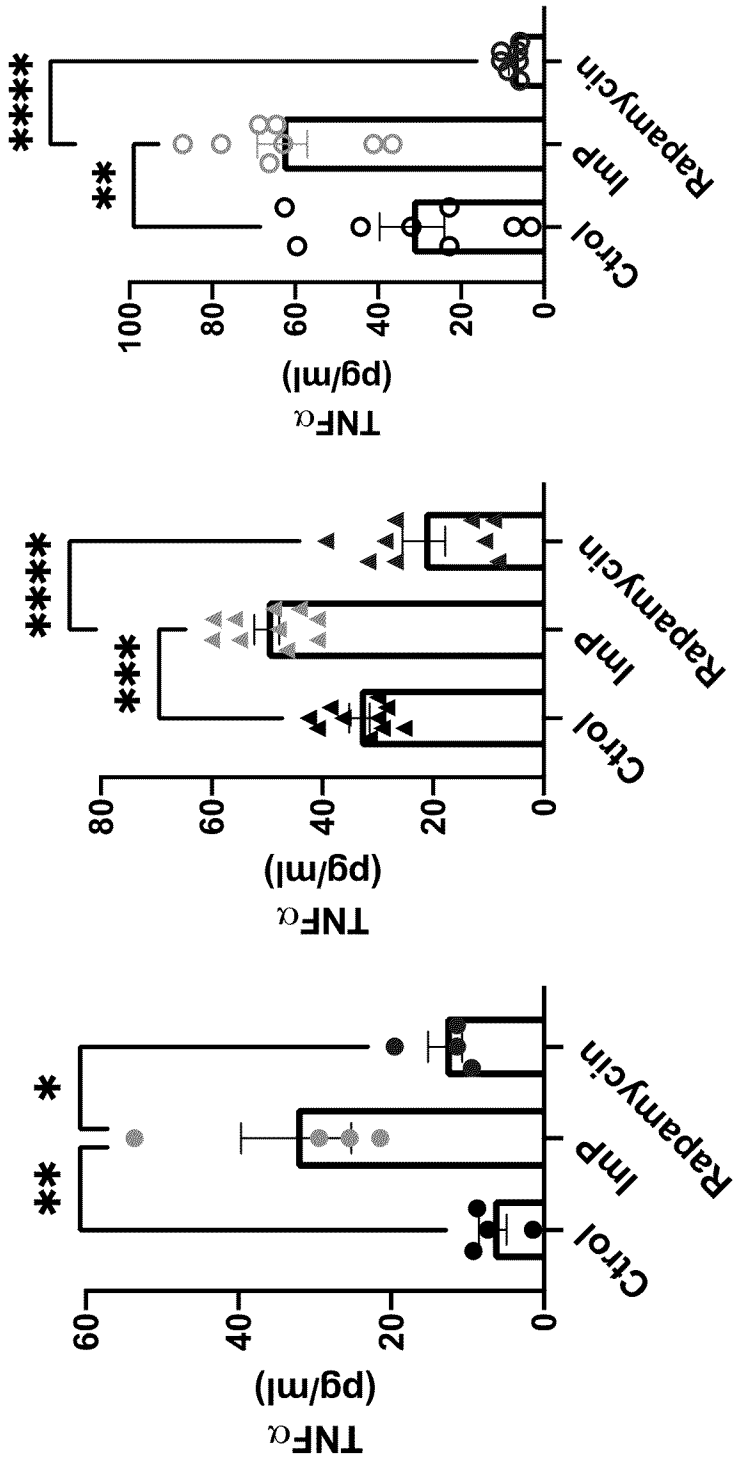

Figure 5a

Figure 5

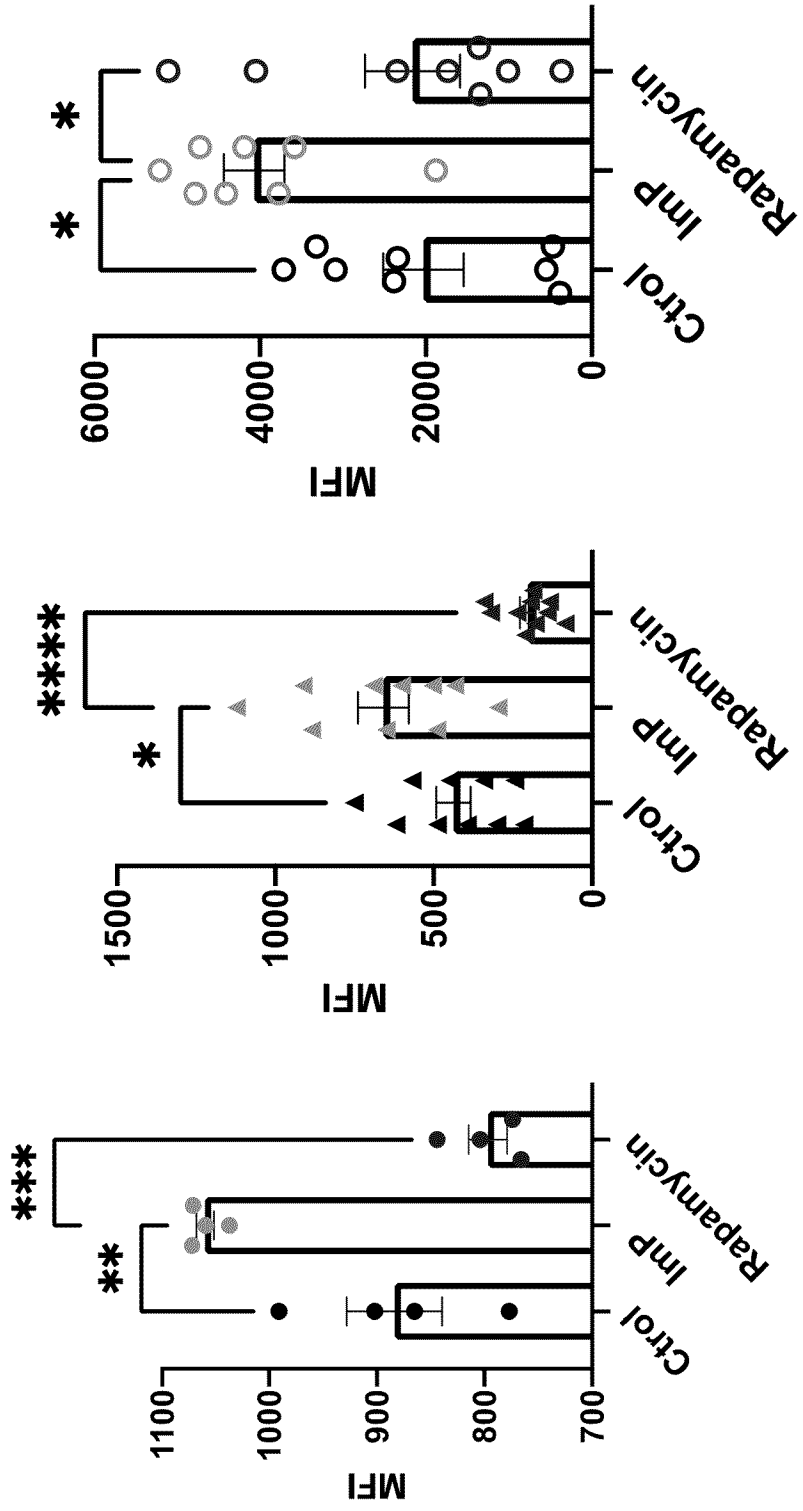
MFI
6000
4000
2000
0
Ctrol
Imp
Rapamycin
*
*
MFI
1500
1000
500
0
Ctrol
Imp
Rapamycin
*
*****
MFI
1100
1000
900
800
700
Ctrol
Imp
Rapamycin
**
****

Figure 5b

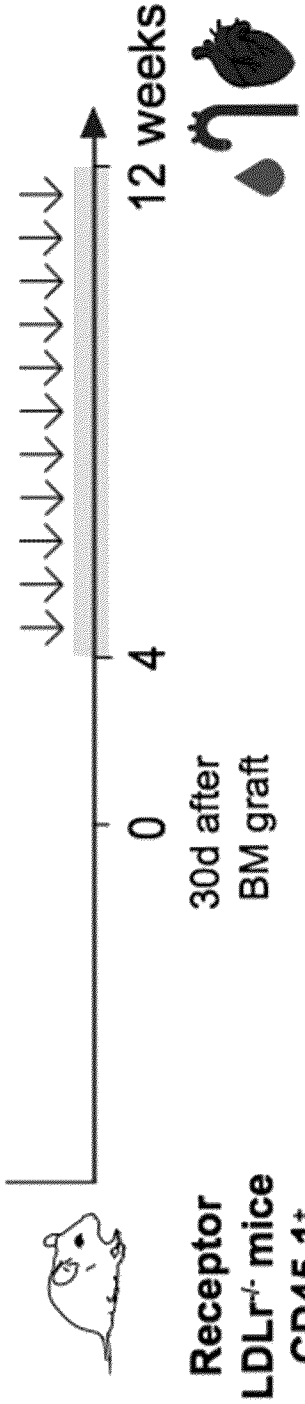
Donor
LysMcre Raptor
CD45.2+
Bone marrow (BM) graft
Receptor
LDLr-/- mice
CD45.1+
0
30d after
BM graft
4
Chow diet +/- ImP
12 weeks

Figure 5c

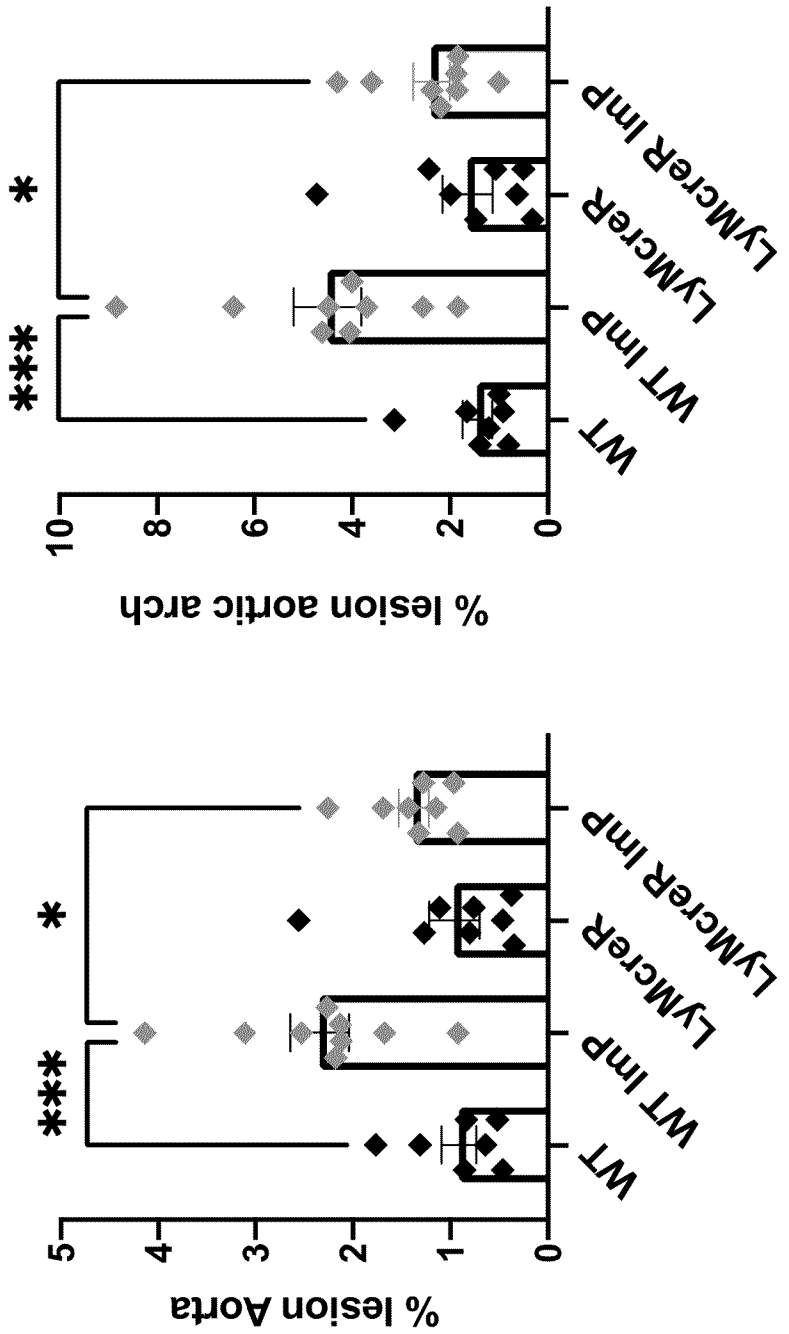
% lesion Aorta
0
1
2
3
4
5
****
*
WT
WT Imp
LyMCreR
LyMCreR Imp
% lesion aortic arch
0
2
4
6
8
10
****
*
WT
WT Imp
LyMCreR
LyMCreR Imp

Figure 5d

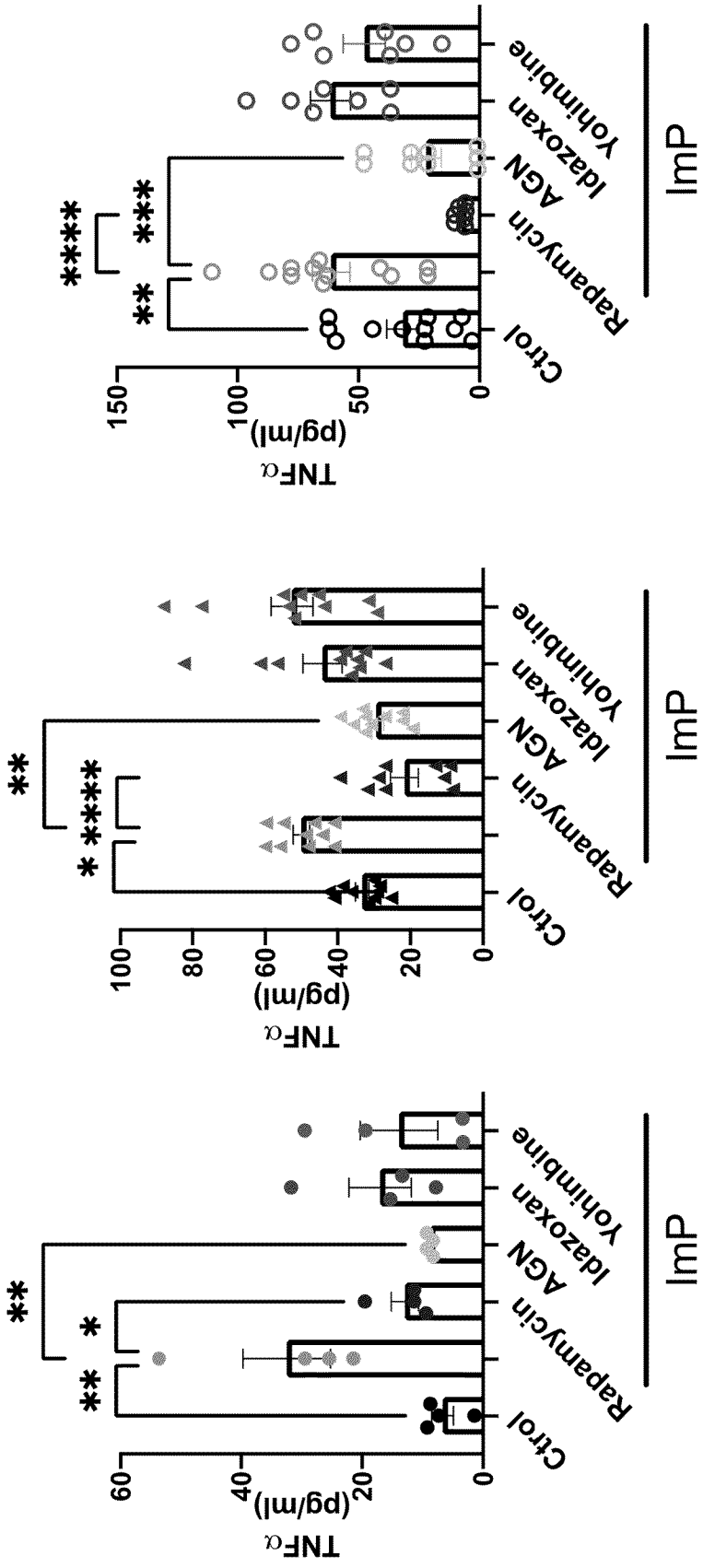

Figure 6

Figure 6a

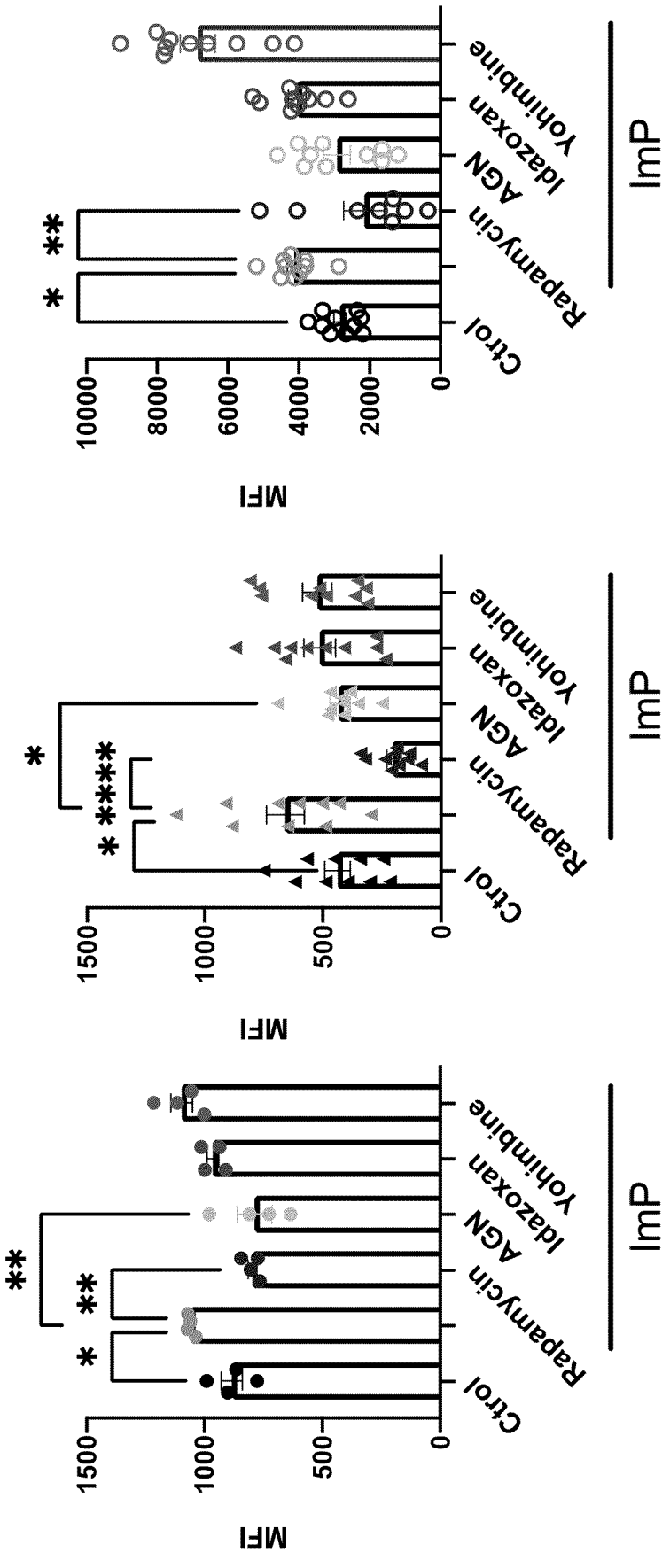
MFI
0
500
1000
1500
Ctrol
Rapamycin
AGN
Idazoxan
Yohimbine
ImP
*
**
***
****
MFI
0
2000
4000
6000
8000
10000
Ctrol
Rapamycin
AGN
Idazoxan
Yohimbine
ImP
*
**

Figure 6b

Figure 7

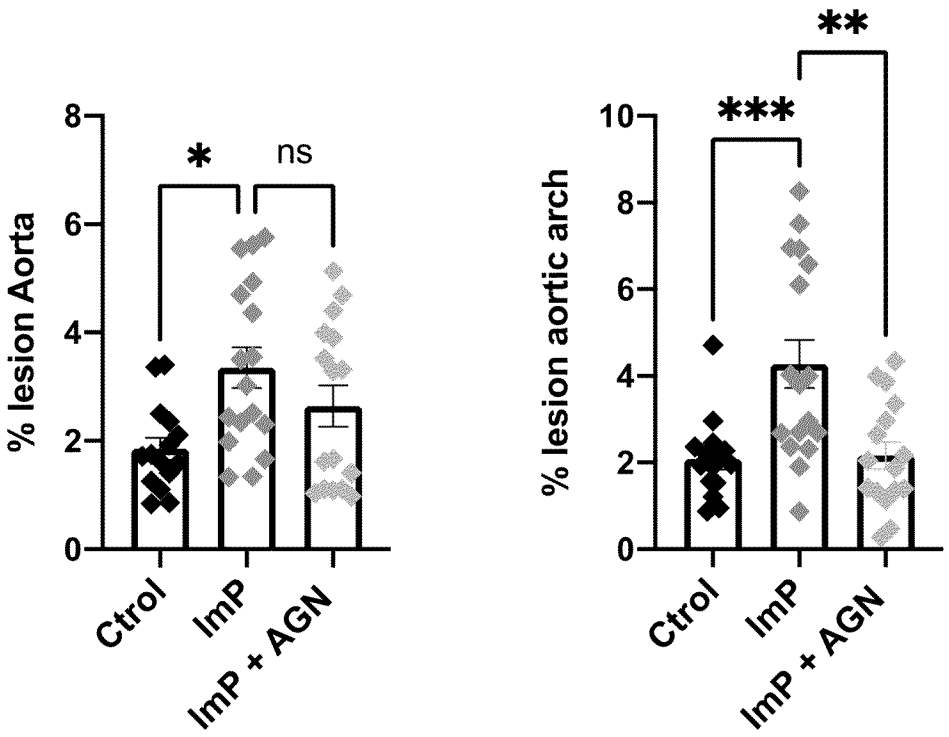

Figure 7a

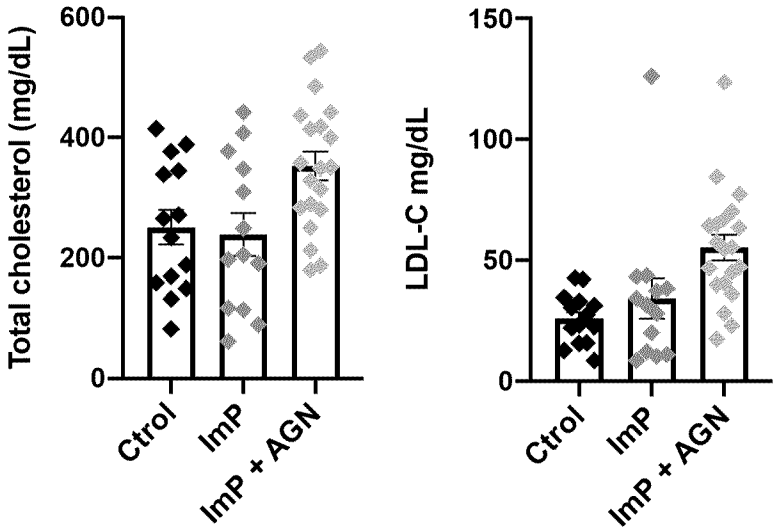

Figure 7b

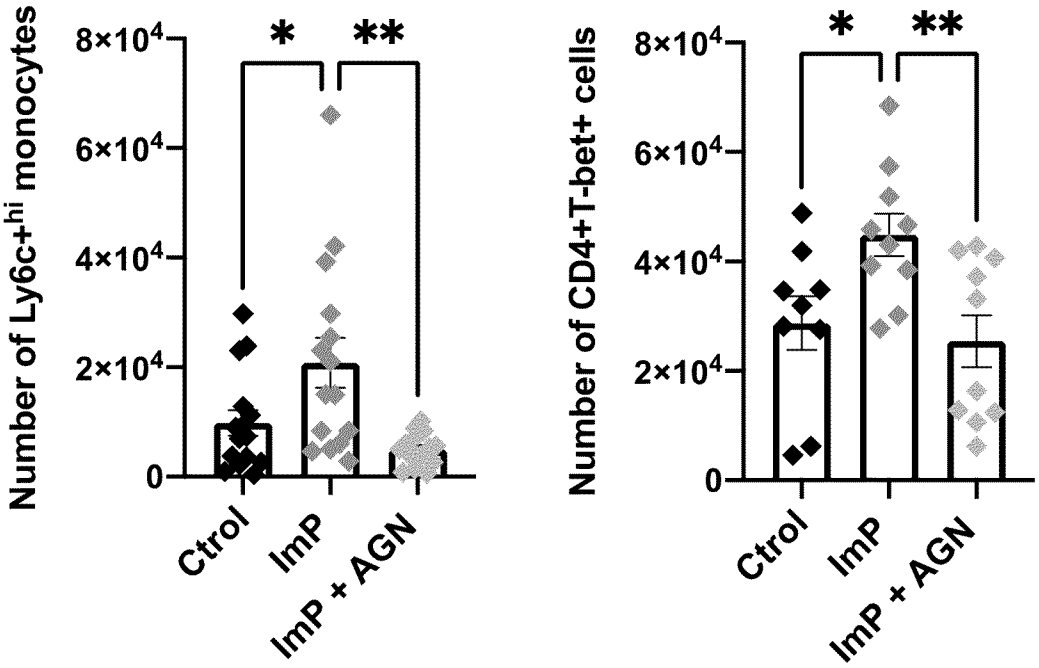

Figure 7c

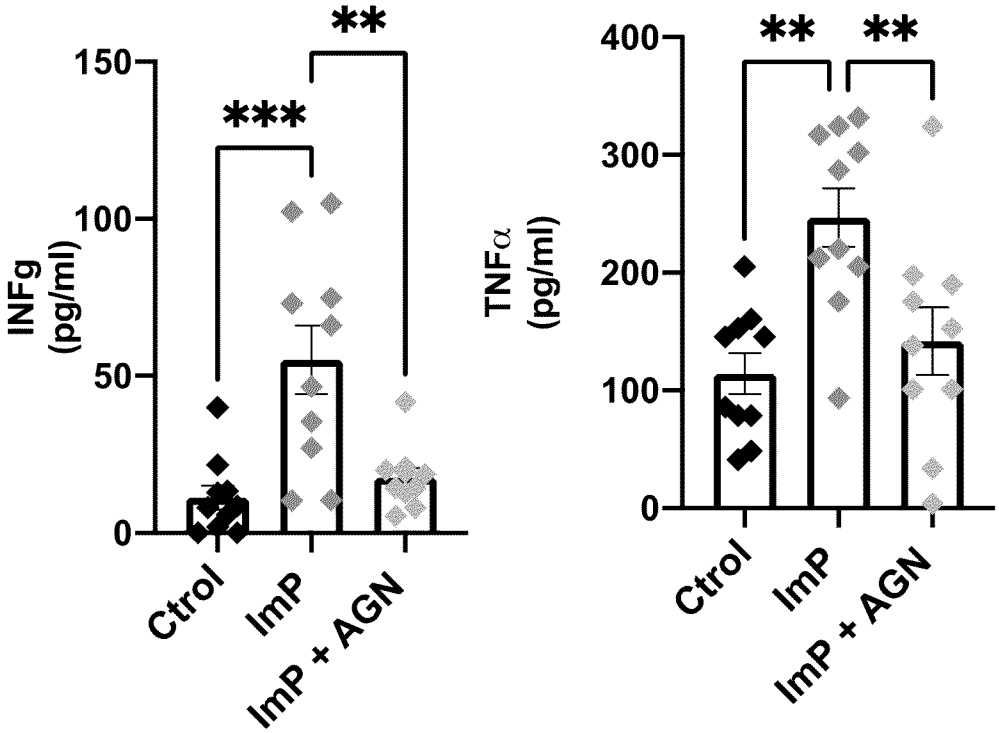

Figure 7d

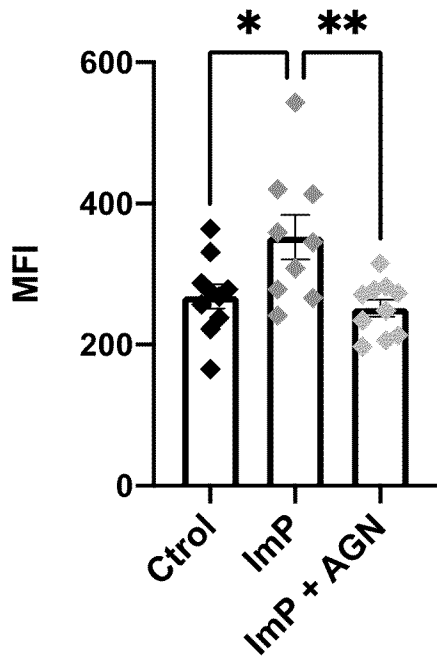

Figure 7e

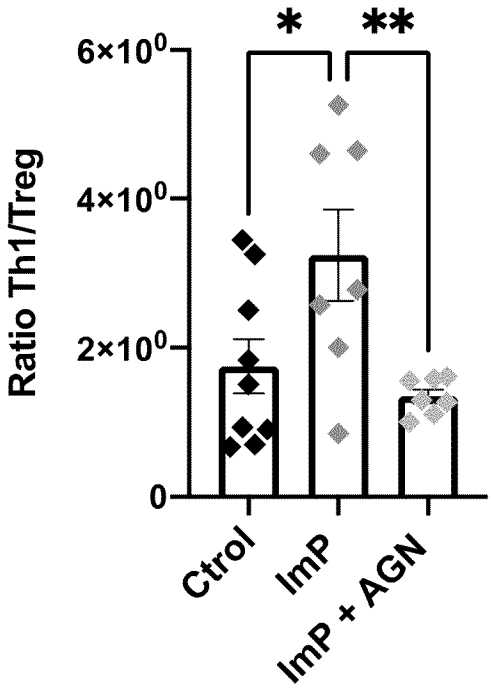

Figure 7f

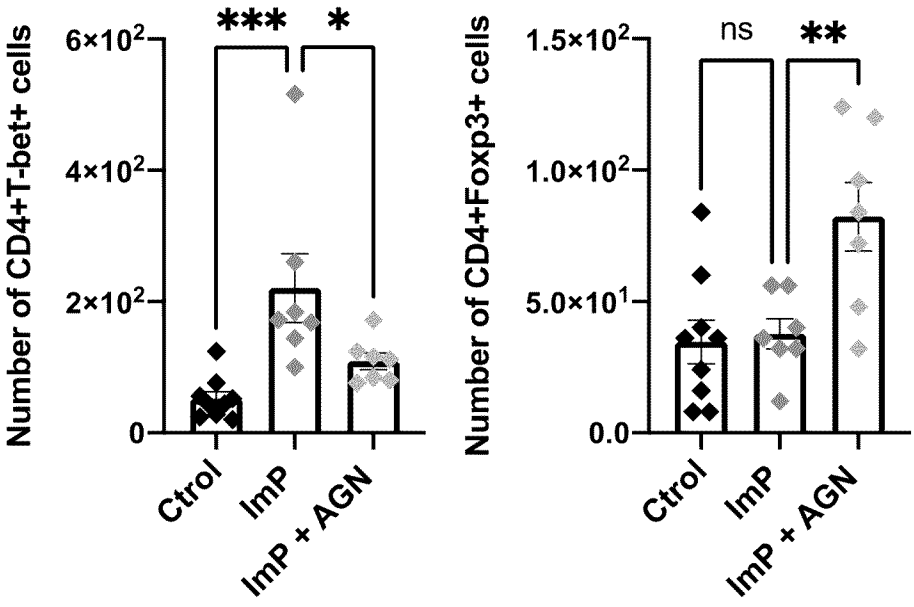

Figure 7g

Figure 8

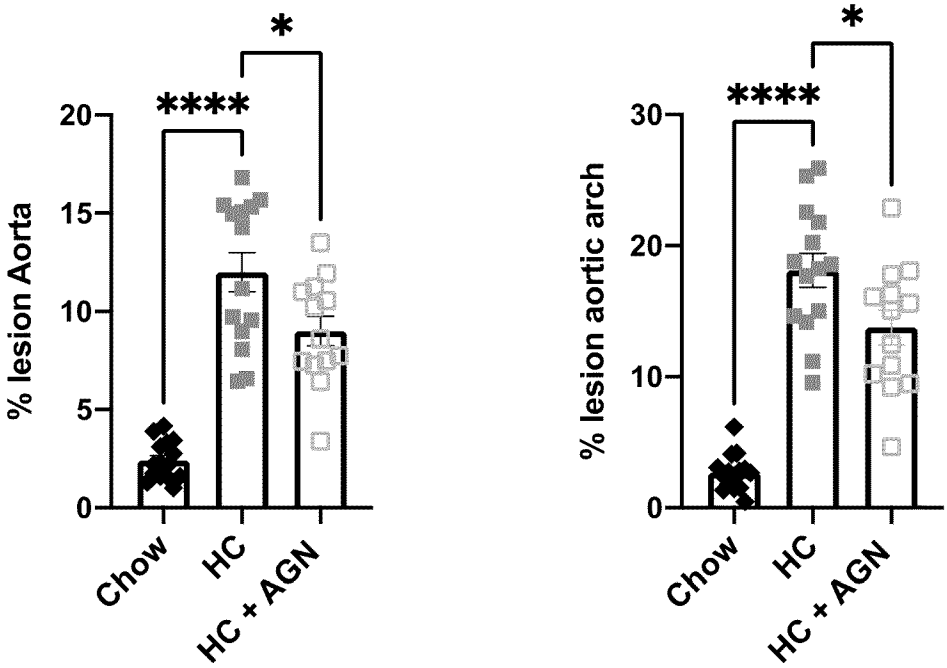

Figure 8a

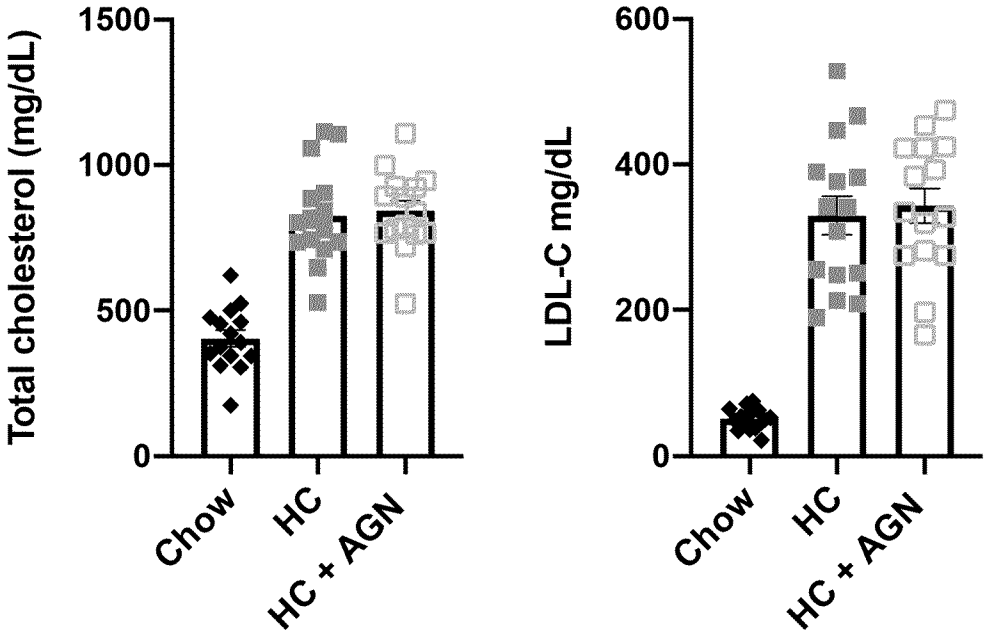

Figure 8b

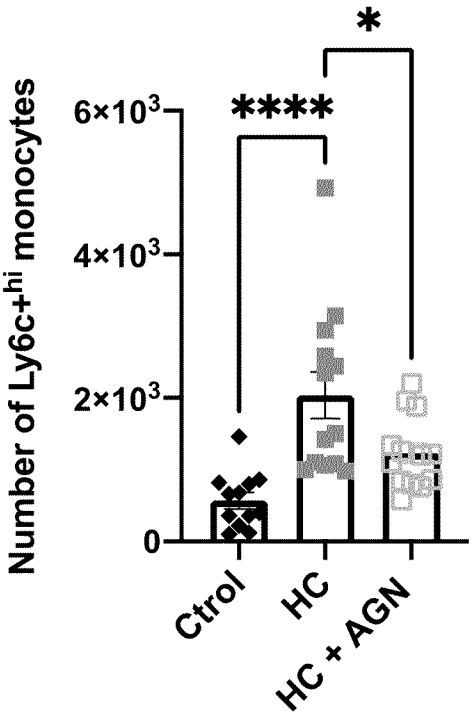

Figure 8c

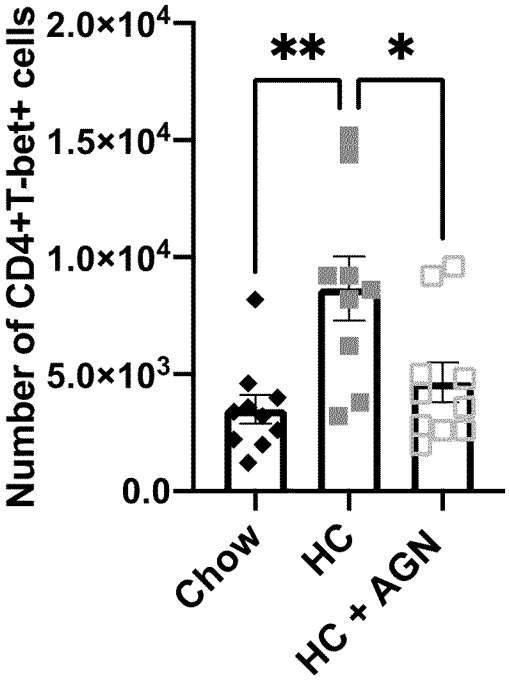

Figure 8d

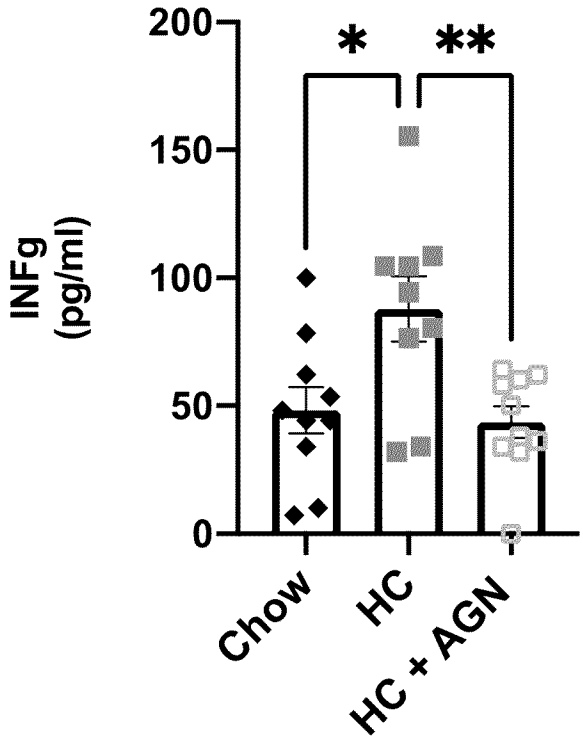

Figure 8e

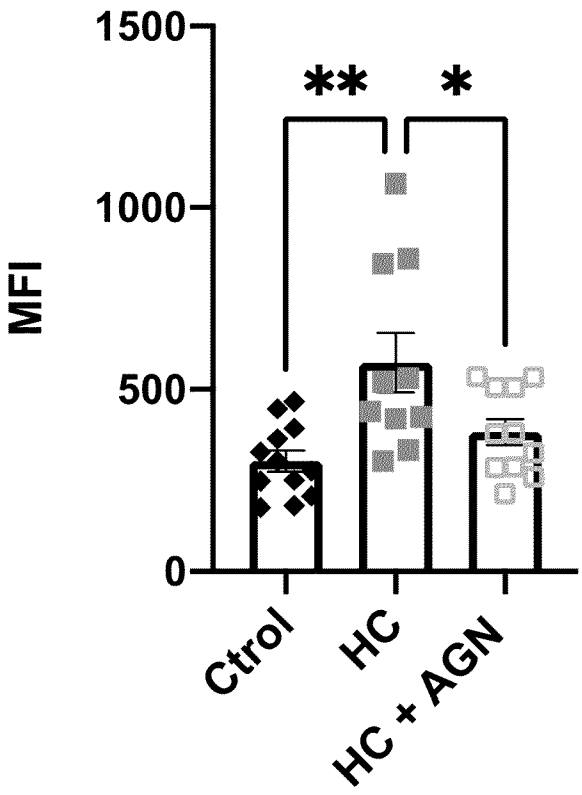

Figure 8f

INTERNATIONAL SEARCH REPORT

International application No.
PCT/EP2024/066950

Box No. II Observations where certain claims were found unsearchable (Continuation of item 2 of first sheet)

This international search report has not been established in respect of certain claims under Article 17(2)(a) for the following reasons:

1. ☐ Claims Nos.:
because they relate to subject matter not required to be searched by this Authority, namely:

2. ☐ Claims Nos.:
because they relate to parts of the international application that do not comply with the prescribed requirements to such an extent that no meaningful international search can be carried out, specifically:

3. ☐ Claims Nos.:
because they are dependent claims and are not drafted in accordance with the second and third sentences of Rule 6.4(a).

Box No. III Observations where unity of invention is lacking (Continuation of item 3 of first sheet)

This International Searching Authority found multiple inventions in this international application, as follows:

see additional sheet

1. ☐ As all required additional search fees were timely paid by the applicant, this international search report covers all searchable claims.

2. ☐ As all searchable claims could be searched without effort justifying an additional fees, this Authority did not invite payment of additional fees.

3. ☐ As only some of the required additional search fees were timely paid by the applicant, this international search report covers only those claims for which fees were paid, specifically claims Nos.:

4. ☒ No required additional search fees were timely paid by the applicant. Consequently, this international search report is restricted to the invention first mentioned in the claims;; it is covered by claims Nos.:
1-6

Remark on Protest

☐ The additional search fees were accompanied by the applicant's protest and, where applicable, the payment of a protest fee.

☐ The additional search fees were accompanied by the applicant's protest but the applicable protest fee was not paid within the time limit specified in the invitation.

☐ No protest accompanied the payment of additional search fees.

INTERNATIONAL SEARCH REPORT

International application No
PCT/EP2024/066950

A. CLASSIFICATION OF SUBJECT MATTER

INV. A61K31/13 A61K31/40 A61K31/428 A61K31/4725 A61P9/10
ADD.

According to International Patent Classification (IPC) or to both national classification and IPC

B. FIELDS SEARCHED

Minimum documentation searched (classification system followed by classification symbols)

A61K A61P

Documentation searched other than minimum documentation to the extent that such documents are included in the fields searched

Electronic data base consulted during the international search (name of data base and, where practicable, search terms used)

EPO-Internal, WPI Data, BIOSIS, CHEM ABS Data, EMBASE

C. DOCUMENTS CONSIDERED TO BE RELEVANT

Category*	Citation of document, with indication, where appropriate, of the relevant passages	Relevant to claim No.
A	ZHENG WANG ET AL: "Gut microbiota, circulating inflammatory markers and metabolites, and carotid artery atherosclerosis in HIV infection", MICROBIOME, BIOMED CENTRAL LTD, LONDON, UK, vol. 11, no. 1, 27 May 2023 (2023-05-27), pages 1-16, XP021319239, DOI: 10.1186/S40168-023-01566-2 abstract	1-6

-/--

[x] Further documents are listed in the continuation of Box C.

[x] See patent family annex.

* Special categories of cited documents :

"A" document defining the general state of the art which is not considered to be of particular relevance

"E" earlier application or patent but published on or after the international filing date

"L" document which may throw doubts on priority claim(s) or which is cited to establish the publication date of another citation or other special reason (as specified)

"O" document referring to an oral disclosure, use, exhibition or other means

"P" document published prior to the international filing date but later than the priority date claimed

"T" later document published after the international filing date or priority date and not in conflict with the application but cited to understand the principle or theory underlying the invention

"X" document of particular relevance;; the claimed invention cannot be considered novel or cannot be considered to involve an inventive step when the document is taken alone

"Y" document of particular relevance;; the claimed invention cannot be considered to involve an inventive step when the document is combined with one or more other such documents, such combination being obvious to a person skilled in the art

"&" document member of the same patent family

Date of the actual completion of the international search	Date of mailing of the international search report
26 August 2024	30/10/2024

Name and mailing address of the ISA/	Authorized officer
European Patent Office, P.B. 5818 Patentlaan 2 NL - 2280 HV Rijswijk Tel. (+31-70) 340-2040, Fax: (+31-70) 340-3016	Garabatos-Perera, J

1

Form PCT/ISA/210 (second sheet) (April 2005)

C(Continuation). DOCUMENTS CONSIDERED TO BE RELEVANT

Category*	Citation of document, with indication, where appropriate, of the relevant passages	Relevant to claim No.
A	Sayols-Baixeras Sergi ET AL: "Streptococcus species abundance in the gut is linked to subclinical coronary atherosclerosis in 8973 participants from the SCAPIS cohort", medRxiv, 2 May 2023 (2023-05-02), pages 1-40, XP093102608, DOI: 10.1101/2022.05.25.22275561 Retrieved from the Internet: URL:https://www.medrxiv.org/content/10.1101/2022.05.25.22275561v3.full.pdf [retrieved on 2023-11-16] abstract	1-6
X	VENTECLEF N ET AL: "The imidazoline-like drug S23515 affects lipid metabolism in hepatocyte by inhibiting the oxidosqualene:lanosterol cyclase activity", BIOCHEMICAL PHARMACOLOGY, ELSEVIER, US, vol. 69, no. 7, 1 April 2005 (2005-04-01), pages 1041-1048, XP027715578, ISSN: 0006-2952 [retrieved on 2005-04-01] abstract page 1046; table 1 page 1041, right-hand column, last paragraph - page 1042, left-hand column, paragraph 3 page 1047, left-hand column, paragraph 2 - right-hand column, paragraph 1	1,5,6
Y	WO 2016/105448 A1 (RIDEOUT DARRYL [US]; LEDERMAN SETH [US] ET AL.) 30 June 2016 (2016-06-30) abstract page 209, last paragraph page 193, lines 15-26 claims 4,44,51	1-6
A	WO 2016/105449 A1 (LEDERMAN SETH [US]; DAUGHERTY BRUCE [US]) 30 June 2016 (2016-06-30) abstract claims compounds 3,43,50 page 48, lines 5-18 page 64, lines 8-17	1-6

-/--

1

C(Continuation). DOCUMENTS CONSIDERED TO BE RELEVANT

Category*	Citation of document, with indication, where appropriate, of the relevant passages	Relevant to claim No.
A	LUMB P J ET AL: "Effect of moxonidine on lipid subfractions in patients with hypertension", INTERNATIONAL JOURNAL OF CLINICAL PRACTICE, MEDICON INTERNATIONAL, ESHER, GB, vol. 58, no. 5, 28 May 2004 (2004-05-28), pages 465-468, XP072058798, ISSN: 1368-5031, DOI: 10.1111/J.1368-5031.2004.00158.X abstract	1-6
A	NIU C-S. ET AL: "A Novel Mechanism for Decreasing Plasma Lipid Level from Imidazoline I-1 Receptor Activation in High Fat Diet-fed Mice", HORMONE AND METABOLIC RESEARCH , vol. 43, no. 07 1 June 2011 (2011-06-01), pages 458-463, XP093102938, DE ISSN: 0018-5043, DOI: 10.1055/s-0031-1275325 Retrieved from the Internet: URL:http://dx.doi.org/10.1055/s-0031-12753 25 abstract	1-6
A	US 5 977 121 A (MEST HANS JUERGEN [DE]) 2 November 1999 (1999-11-02) abstract claims	1-6
Y	HEAD G. ET AL: "Imidazoline Receptors, Novel Agents and Therapeutic Potential", CARDIOVASCULAR & HEMATOLOGICAL AGENTS IN MEDICINAL CHEMISTRY, vol. 4, no. 1, 1 January 2006 (2006-01-01) , pages 17-32, XP093102414, NL ISSN: 1871-5257, DOI: 10.2174/187152506775268758 abstract page 25, left-hand column, line 3 - right-hand column, paragraph 2	1-6

1

INTERNATIONAL SEARCH REPORT

Information on patent family members

International application No
PCT/EP2024/066950

Patent document cited in search report	Publication date	Patent family member(s)	Publication date
WO 2016105448 A1	30-06-2016	NONE	
WO 2016105449 A1	30-06-2016	NONE	
US 5977121 A	02-11-1999	AU 4941796 A	18-09-1996
		CA 2212294 A1	06-09-1996
		EP 0812197 A2	17-12-1997
		JP H11501020 A	26-01-1999
		KR 19980702511 A	15-07-1998
		US 5977121 A	02-11-1999
		WO 9626728 A2	06-09-1996

FURTHER INFORMATION CONTINUED FROM PCT/ISA/ 210

This International Searching Authority found multiple (groups of) inventions in this international application, as follows:

1. claims: 1-6

   Antagonists of imidazoline-1 receptor (I1 R) (i.e. AGN192403, S23757, LNP911, BU98008, S23515, and benazoline) for use in the prevention and/or treatment of an autoinflammatory or autoimmune disease and related subject-matter.

   ---

2. claim: 7

   Methods for screening and/or producing therapeutic candidates for the prevention and/or treatment of an autoinflammatory or autoimmune disease.

   ---

3. claims: 8-13

   Use of imidazole propionate (ImP) in the diagnosis of an autoinflammatory or autoimmune disease and related subject-matter.
